
BRINGING DIFFERENTIAL PRIVATE SGD TO PRACTICE: ON THE INDEPENDENCE OF GAUSSIAN NOISE AND THE NUMBER OF TRAINING ROUNDS

Marten van Dijk^{1,2*}, **Nhuong V. Nguyen**^{3†*}, **Toan N. Nguyen**^{3†},
Lam M. Nguyen⁴, **Phuong Ha Nguyen**⁵

¹ CWI Amsterdam, The Netherlands

² Department of Electrical and Computer Engineering, University of Connecticut, CT, USA

³ Department of Computer Science and Engineering, University of Connecticut, CT, USA

⁴ IBM Research, Thomas J. Watson Research Center, Yorktown Heights, NY, USA

⁵ eBay, CA, USA

marten.van.dijk@cwi.nl, nhuong.nguyen@uconn.edu, toan.nguyen@uconn.edu,
LamNguyen.MLTD@ibm.com, phuongha.ntu@gmail.com

ABSTRACT

In the context of DP-SGD each round communicates a local SGD update which leaks some new information about the underlying local data set to the outside world. In order to provide privacy, Gaussian noise is added to local SGD updates. However, privacy leakage still aggregates over multiple training rounds. Therefore, in order to control privacy leakage over an increasing number of training rounds, we need to increase the added Gaussian noise per local SGD update. This dependence of the amount of Gaussian noise σ on the number of training rounds T may impose an impractical upper bound on T (because σ cannot be too large) leading to a low accuracy global model (because the global model receives too few local SGD updates). DP-SGD much less competitive compared to other existing privacy techniques.

We show for the first time that for (ϵ, δ) -differential privacy σ can be chosen equal to $\sqrt{2(\epsilon + \ln(1/\delta))/\epsilon}$ regardless the total number of training rounds T . In other words, σ does not depend on T anymore (and aggregation of privacy leakage increases to a limit). This important discovery brings DP-SGD to practice because σ can remain small to make the trained model have high accuracy even for large T as usually happens in practice.

1 Introduction

The optimization problem for training many Machine Learning (ML) models using a training set $\{\xi_i\}_{i=1}^m$ of m samples can be formulated as a finite-sum minimization problem as follows

$$\min_{w \in \mathbb{R}^d} \left\{ F(w) = \frac{1}{m} \sum_{i=1}^m f(w; \xi_i) \right\}. \quad (1)$$

The objective is to minimize a loss function with respect to model parameters w . This problem is known as empirical risk minimization and it covers a wide range of convex and non-convex problems from the ML domain, including, but not limited to, logistic regression, multi-kernel learning, conditional random fields and neural networks.

* these authors contributed equally.

† supported by NSF grant CNS-1413996 “MACS: A Modular Approach to Cloud Security.”

We want to solve (1) in a distributed setting where many clients have their own local data sets and the finite-sum minimization problem is over the collection of all local data sets. A widely accepted approach is to repeatedly use the Stochastic Gradient Descent (SGD) recursion

$$w_{t+1} = w_t - \eta_t \nabla f(w_t; \xi), \quad (2)$$

where w_t represents the model after the t -th iteration; w_t is used in computing the gradient of $f(w_t; \xi)$, where ξ is a data sample randomly selected from the data set $\{\xi_i\}_{i=1}^m$ which comprises the union of all local data sets.

This approach allows each client to perform local SGD recursions for the ξ that belong to the client’s local data set. The updates as a result of the SGD recursion (2) are sent to a centralized server who aggregates all received updates and maintains a global model. The server regularly broadcasts its most recent global model so that clients can use it in their local SGD computations. This allows each client to use what has been learned from the local data sets at the other clients. This leads to good accuracy of the final global model.

Each client is doing SGD recursions for a batch of local data. These recursions together represent a local round and at the end of the local round the sum of local model updates, i.e., the addition of computed gradients, is transmitted to the server. The server in turn adds the received sum of local updates to its global model – and once the server receives new sums from all clients, the global model is broadcast to each of the clients. When considering privacy, we are concerned about how much information these sums of local updates reveal about the used local data sets. Each client wants to keep its local data set as private as possible with respect to the outside world which observes round communication (the outside world includes all other clients as well).

Rather than reducing the amount of round communication such that less sensitive information is leaked, differential privacy [Dwork et al., 2006b, Dwork, 2011, Dwork et al., 2014, 2006a] offers a solution in which each client-to-server communication is obfuscated by noise. If the magnitude of the added noise is not too much, then a good accuracy of the global model can still be achieved albeit at the price of more overall SGD iterations needed for achieving good accuracy. On the other hand, only if the magnitude of the added noise is large enough, then good differential privacy guarantees can be given.

We notice that aggregated privacy leakage of the local data set over the total number of rounds from a differential privacy perspective is not the same as measuring aggregated privacy leakage from a Shannon entropy perspective. Nevertheless, in order to *gain more understanding**, we proceed analysing aggregated privacy leakage from a Shannon entropy perspective: Let random variable L_i denote the observed information about the local data set that is present in the noisy local SGD update communicated to the central server in round i . Then the total amount of Shannon information present in the aggregated leakage $L_0 L_1 \dots L_{T-1}$ is equal to (by $H(\cdot)$ we denote Shannon entropy)

$$H(L_0 L_1 \dots L_{T-1}) = \sum_{i=0}^{T-1} H(L_i | L_0 \dots L_{i-1}). \quad (3)$$

This shows that even though round i leaks $H(L_i)$ bits of information, the aggregated leakage increments with $H(L_i | L_0 \dots L_{i-1})$ bits in round i . This is generally less than $H(L_i)$ because L_i contains information that was already contained in the leakage $L_0 \dots L_{i-1}$ of the prior rounds. As of yet it is unclear whether the sum in (3) increases in T to a limit H^* or is unbounded (∞).

As discussed in [Abadi et al., 2016], in order to control privacy leakage over an increasing number of training rounds, we need to increase the magnitude, or standard deviation σ , of the added noise per round. In the Shannon entropy setting, increasing σ makes each $H(L_i)$ smaller and as a result the entries in sum (3) become smaller, and the aggregated leakage becomes less. For a fixed privacy leakage budget this allows us to add more entries, in other words, we may increase T . The maximum possible T increases as σ increases.

This dependence of the amount of Gaussian noise σ on the number of training rounds T may impose an impractical upper bound on T : First, σ cannot be too large. The global model suffers from aggregated noise from each local update. In particular, the global model includes σ noise from the final training round. If σ is too large, then this leads to a low accuracy global model. Second, if σ cannot be too large, then the number of training rounds T cannot be too large because otherwise privacy leakage aggregates too much over all training rounds. But this implies that the global model may receive too few local SGD updates; local SGD updates from different clients are communicated through the global model to one another using too few interactions/rounds (frequent exchange is especially important when local data sets are heterogeneous, hence, different clients produce distinctive updates that are specific to their local data sets). This leads again to a low accuracy global model. This intuition/reasoning indicates that Differential Private SGD (DP-SGD) can only be practical for subtle parameter settings and data sets that allow ‘fast enough’ training/convergence to a good

*Our main Theorem 2 only uses reasoning based on differential privacy and cannot be used to conclude the Shannon entropy arguments presented here.

accuracy global model. In general, DP-SGD is expected to be much less competitive compared to using other existing privacy techniques (such as secure multiparty computation even though this is less efficient).

Main intuition and motivation. The above reasoning holds ground if the aggregated privacy leakage steadily increments with the total number T of training rounds in that (3) is unbounded for increasing T . However, if the leakage increments $H(L_i|L_0 \dots L_{i-1})$ become smaller and smaller, then, even though aggregated leakage increases, it may reach a limit H^* (i.e., (3) has a limit H^* for increasing T). If true, this suggests that we may choose σ to be *independent* of T to accommodate this limit: Limit H^* will be a function of σ which decreases for increasing σ (since increasing σ will reduce each $H(L_i)$). So, in order to remain within a certain privacy leakage budget B , we need to choose σ large enough so that the corresponding limit $H^*(\sigma)$ is at most our budget B . Once σ is chosen such that $H^*(\sigma) \leq B$, we remain within our privacy leakage budget for any choice of T : This is because any choice of T yields a sum (3) which is at most our limit $H^*(\sigma)$ (of (3) for $T \rightarrow \infty$), which is in turn at most our budget B . In this paper we answer in the affirmative that this intuition is also valid from the differential privacy perspective, where (ϵ, δ) in (ϵ, δ) -differential privacy can be thought of as our privacy budget " B ":

Main contribution. We show for the first time that (ϵ, δ) -differential privacy can be achieved for σ equal to $\sqrt{2(\epsilon + \ln(1/\delta))}/\epsilon$ regardless the total number of training rounds T . In other words, σ does not depend on T anymore. This important discovery brings DP-SGD to practice because σ can remain small to make the trained model have high accuracy even for large T as happens in practice.

Outline. In order to set up the proper background, we first discuss differential privacy in Section 2, next discuss DP-SGD as introduced by Abadi et al. [Abadi et al., 2016] in Section 3, and explain in Section 4 that according to their analysis/theory the maximum number of local training rounds is significantly restricted. In relation to this, we detail discuss the independence of σ and T in Section 5, i.e., we explain that there is no ceiling to the total number of local training rounds in DP-SGD and that this can be chosen independent of the required differential privacy with corresponding Gaussian noise. Our main theorems are in Section 6 with experiments in Section 7.

2 Differential Privacy

Differential privacy [Dwork et al., 2006b, Dwork, 2011, Dwork et al., 2014, 2006a] defines privacy guarantees for algorithms on databases, in our case a client's sequence of mini-batch gradient computations on his/her training data set. The guarantee quantifies into what extent the output of a client (the collection of updates communicated to the server) can be used to differentiate among two adjacent training data sets d and d' (i.e., where one set has one extra element compared to the other set).

Definition 1. A randomized mechanism $\mathcal{M} : D \rightarrow R$ is (ϵ, δ) -DP (Differentially Private) if for any adjacent d and d' in D and for any subset $S \subseteq R$ of outputs,

$$Pr[\mathcal{M}(d) \in S] \leq e^\epsilon Pr[\mathcal{M}(d') \in S] + \delta,$$

where the probabilities are taken over the coin flips of mechanism \mathcal{M} .

The privacy loss incurred by observing o is given by

$$L_{\mathcal{M}(d) \parallel \mathcal{M}(d')}^o = \ln \left(\frac{Pr[\mathcal{M}(d) = o]}{Pr[\mathcal{M}(d') = o]} \right).$$

As explained in [Dwork et al., 2014] (ϵ, δ) -DP ensures that for all adjacent d and d' the absolute value of privacy loss will be bounded by ϵ with probability at least $1 - \delta$. The larger ϵ the more certain we are about which of d or d' caused observation o . When using differential privacy in machine learning we typically use $\delta = 1/N$ (or $1/(10N)$) inversely proportional with the data set size N .

In order to prevent data leakage from inference attacks in machine learning [Lyu et al., 2020] such as the deep leakage from gradients attack [Zhu et al., 2019, Zhao et al., 2020, Geiping et al., 2020] or the membership inference attack [Shokri et al., 2017, Nasr et al., 2019, Song et al., 2019] a range of privacy-preserving methods have been proposed. Privacy-preserving solutions for federated learning are Local Differential Privacy (LDP) solutions [Abadi et al., 2016, Bhowmick et al., 2019, Naseri et al., 2021, Truex et al., 2019, Hao et al., 2020, Duchi et al., 2014] and Central Differential Privacy (CDP) solutions [Naseri et al., 2021, Geyer et al., 2018, McMahan et al., 2018, Papernot et al., 2018, Yu et al., 2019]. In LDP, the noise for achieving differential privacy is computed locally at each client and is added to the updates before sending to the server – in this paper we also consider LDP. In CDP, a trusted server aggregates received client updates into a global model; in order to achieve differential privacy the server adds noise to the global model before communicating it to the clients.

3 Differential Private SGD (DP-SGD)

In this paper we analyse the Gaussian based differential privacy method, called DP-SGD, of [Abadi et al., 2016], depicted in Algorithm 1. Rather than using the gradient $\nabla f(\hat{w}, \xi)$ itself, DP-SGD uses its clipped version $[\nabla f(\hat{w}, \xi)]_C$ where $[x]_C = x / \max\{1, \|x\|/C\}$. Clipping is needed because in general we cannot assume a bound C on the gradients (for example, the bounded gradient assumption is in conflict with strong convexity [Nguyen et al., 2018]), yet the added gradients need to be bounded by some constant C in order for the DP analysis of [Abadi et al., 2016] to go through. Experiments in [Abadi et al., 2016] show that such a clipped version of mini-batch SGD still leads to acceptable convergence to acceptable accuracy.

DP-SGD uses a mini-batch approach where before the start of the i -th local round a random min-batch of sample size s_i is selected out of a local data set d of size $|d| = N$. Here, we slightly generalize DP-SGD’s original formulation which uses a constant $s_i = s$ sample size sequence, while our analysis will hold for a larger class of sample size sequences. The inner loop maintains the sum U of gradient updates where each of the gradients correspond to the same local model \hat{w} until it is replaced by a newer global model at the start of the outer loop. At the end of each local round the sum of updates U is obfuscated with Gaussian noise $\mathcal{N}(0, C^2 \sigma^2)$ added to each vector entry, and the result is transmitted to the server. The noised U is transmitted to the server who adds U times the round step size $\bar{\eta}_i$ to its global model \hat{w} . As soon as all clients have submitted their updates, the resulting new global model \hat{w} is broadcast to all clients, who in turn replace their local models with the newly received global model (at the start of the outer loop).

Algorithm 1 DP-SGD: Local Model Updates with Differential Privacy

```

1: procedure LOCALSGDWITHDP( $d$ )
2:   for  $i \in \{0, \dots, T - 1\}$  do
3:     Receive the current global model  $\hat{w}$  from the Server.
4:     Uniformly sample a random set  $\{\xi_h\}_{h=1}^{s_i} \subseteq d$ 
5:      $h = 0, U = 0$ 
6:     while  $h < s_i$  do
7:        $g = [\nabla f(\hat{w}, \xi_h)]_C$ 
8:        $U = U + g$ 
9:        $h++$ 
10:    end while
11:     $n \leftarrow \mathcal{N}(0, C^2 \sigma^2 \mathbf{I})$ 
12:     $U = U + n$ 
13:    Send  $(i, U)$  to the Server.
14:  end for
15: end procedure

```

4 DP-SGD Analysis by Abadi et al. [Abadi et al., 2016]

Abadi et al. [Abadi et al., 2016] prove the following theorem (rephrased using our notation with $q = s/N$):

Theorem 1. *There exist constants c_1 and c_2 so that given a sample size sequence $s_i = s$ and number of steps T , for any $\epsilon < c_1 T (s/N)^2$, Algorithm 1 is (ϵ, δ) -differentially private for any $\delta > 0$ if we choose*

$$\sigma \geq c_2 \frac{(s/N) \cdot \sqrt{T \ln(1/\delta)}}{\epsilon}.$$

The theorem suggests a necessary dependence between σ and T where σ scales with \sqrt{T} for fixed s and N . If this is indeed necessary, then in order to achieve good accuracy for a given σ we need to increase the number of rounds T , but this requires us to increase σ , which increases T , etc. This reasoning would imply a subtle setting of σ and T for a given privacy budget (ϵ, δ) that leads to ‘best’ accuracy. Here, σ must be small enough so that it does not cause too much noise in the final global model. But this implies that the ‘best’ accuracy is restricted by only being able to use a limited number of training rounds T (since T cannot be too large for small enough $\sigma = O(\sqrt{T})$).

The interpretation of Theorem 1, however, is more subtle: The condition on ϵ in Theorem 1 is equivalent to

$$1/\sqrt{c_1} < z \text{ where } z = (s/N) \cdot \sqrt{T/\epsilon}.$$

Substituting this into the bound for σ yields

$$\sigma \geq (c_2 \cdot z) \cdot \sqrt{\frac{\ln(1/\delta)}{\epsilon}}. \tag{4}$$

This formulation only depends on T through the definition of z . Notice that z may be as small as $1/\sqrt{c_1}$. In fact, it is unclear how z depends on T since T is equal to the total number K of gradient computations over all local rounds performed on the local data set divided by the mini-batch size s , i.e., $T = K/s$, hence, $z = (K/N) \cdot \sqrt{1/(T\epsilon)}$. This shows that for fixed K and N , we can increase T as long as $1/\sqrt{c_1} < z$, or equivalently,

$$T < c_1(K/N)^2/\epsilon \quad (5)$$

(notice that the original constraint on ϵ in Theorem 1 directly translates into this upper bound on T by using $T = K/s$). Since σ cannot be chosen too large (otherwise the final global model has too much noise), ϵ , see (4), cannot be very small (like $\epsilon \approx 0.001$). Therefore, this more precise analysis still puts an upper bound on T which is in general much less than K (for practically sized large data sets), the maximum possible number of rounds for mini-batch size $s = 1$.

Rather than applying Theorem 1, we can directly use the moment accountant method of its proof to analyse specific parameter settings. It turns out that T can be much larger than upper bound (5). In this paper we formalize this insight (by showing that ‘constants’ c_1 and c_2 can be chosen as functions of T and other parameters) and show a lower bound on σ which does not depend on T at all – in fact z in (4) can be characterized as a constant independent of any parameters. This will show that σ can remain small up to a lower bound that only depends on the privacy budget. We can freely increase T (up to K if needed) in order to improve accuracy.

5 Independence between σ and T

We go beyond the analysis presented by Abadi et al. [Abadi et al., 2016] in a non-trivial way and show that (ϵ, δ) -DP (Differential Privacy) holds for per round added Gaussian noise with standard deviation (normalized with respect to the clipping constant C)

$$\sigma = \sqrt{\frac{2(\epsilon + \ln(1/\delta))}{\epsilon}} \quad (6)$$

if

$$\sigma \leq \frac{N\sqrt{T}}{K} \sqrt{\frac{2(\epsilon + \ln(1/\delta))}{\gamma\theta^2}}, \quad (7)$$

where γ is some constant ≈ 2 , θ measures the variation in the sample size sequence $\{s_i\}_{i=0}^{T-1}$ used for selecting mini-batches during the local mini-batch SGD computations (constant sample size sequences have $\theta = 1$), T is the number of local rounds, and K is the total number of gradient computations (iterations) over all local rounds performed on the local data set. This compares to taking $c_2 z \approx \sqrt{2}$ in (4). We do have the new constraint (7) which we interpret below.

Interpretation: In general, practical parameter settings that achieve good enough accuracy show that σ must be restricted to at most 10, 20, may be 35 (this depends on the data set). This shows that if $N\sqrt{T}/K$ is large enough, larger than the relatively small $\sigma\sqrt{\theta^2(\gamma/2)/(\epsilon + \ln(1/\delta))}$, then upper bound (7) is satisfied. That is, for given K and N , we need T to be large enough, or equivalently the mean sample/mini-batch size $\bar{s} = K/T$ small enough. Squaring both sides of (7) and moving terms yields the lower bound

$$T \geq \frac{\gamma}{2} \frac{\sigma^2 \theta^2}{\epsilon + \ln(1/\delta)} \cdot (K/N)^2. \quad (8)$$

In other words T is at least a factor $\sigma^2 \theta^2 (\gamma/2) / (\epsilon + \ln(1/\delta))$ larger than the square of the overall amount of local SGD computations measured in epochs (of size N). Notice that we have a lower bound on T rather than an upper bound as in (5).

We notice the natural restriction $T \leq K$ as there can be no more local rounds than the total number of local gradient computations (each mini-batch must at least contain one element). Substituting the maximum K for T in (8) and reordering terms shows that there exists a (large) T satisfying (8) only if $K \leq N^2(\epsilon + \ln(1/\delta))/\sigma^2 \theta^2 (\gamma/2)$. In other words K is at least a constant times N epochs (of N gradient computations each), which is true in any practical parameter setting.

This shows that in practical settings there is no imposed ceiling for T and corresponding to T there is a wide range of accommodating sample size sequences (with $\bar{s} = K/T$). We only need to make sure to choose σ , ϵ , and δ according to (6). Allowable sample size sequences also include polynomial increasing ones with $s_i \approx q \cdot i^p$ which have $\theta = p + 1$. Using such increasing sample size sequences reduces the number of rounds T and, hence, the amount of communication

for a given K . [van Dijk et al., 2020] gives evidence that increasing sample size sequences still lead to sufficient convergence to practical accuracy.

Since (6) does not involve T (or K), (ϵ, δ) -DP is achieved for any increasing number of rounds with the same noise σ . *This is counter intuitive as we expect to see a steady aggregation of leakage from round to round, which after some moment is too much for guaranteeing (ϵ, δ) -DP. This latter intuition is also expressed by Abadi et al. [Abadi et al., 2016] in Theorem 1 and the resulting upper bound (5) on T . Nevertheless, our analysis shows that it suffices to satisfy the weaker constraint (6) with lower bound (8) on T .*

This has a major practical consequence: *If we need to increase T (and K) for achieving convergence to better practical accuracy, then we do not need to increase σ in order to remain guaranteeing differential privacy. Prior to this work the above explained incorrect intuition prevented us from increasing T too much as this would imply (according to this intuition) a too large increase in σ which inherently leads to impractical accuracy.*

One order of magnitude smaller ϵ : In order to attain an accuracy comparable to the non-DP setting where no noise is added, the papers cited in Section 2 generally require large ϵ (such that σ can be small enough) – which gives a weak privacy posture (a weak bound on the privacy loss). For example, when considering LDP (see Section 2), 10% deduction in accuracy yields only $\epsilon = 50$ in [Bhowmick et al., 2019] and $\epsilon = 10.7$ in [Naseri et al., 2021], while [Truex et al., 2019, Hao et al., 2020] show solutions for a much lower $\epsilon = 0.5$. Similarly, when considering CDP (see Section 2), in order to remain close to the accuracy of the non-DP setting [Naseri et al., 2021] requires $\epsilon = 8.1$, [Geyer et al., 2018] requires $\epsilon = 8$, and [McMahan et al., 2018] requires $\epsilon = 2.038$.

The theory presented in this paper allows relatively small Gaussian noise for small ϵ : We only need to satisfy the main equation (6). For example in Section 7 simulations for the LIBSVM data set show $(\epsilon = 0.05, \delta = 1/N)$ -DP is possible while achieving good accuracy with $\sigma \approx 20$. Such small ϵ is a significant improvement over existing literature and gives us significant more trust in that DP offers appropriate privacy.

6 Main DP Theorem

The proof of our main theorem is in Supplemental Material B, where we generalize Theorem 1 in a non-trivial way by analysing increasing sample size sequences, by making explicit the higher order error term in [Abadi et al., 2016], and by providing a precise relationship among the constants c_1 and c_2 in Theorem 1.

Theorem 2. *For sample size sequence $\{s_i\}_{i=0}^{T-1}$ the total number of local SGD iterations is equal to $K = \sum_{i=0}^{T-1} s_i$. We define the mean \bar{s} and maximum s_{max} and their quotient θ as*

$$\bar{s} = \frac{1}{T} \sum_{i=0}^{T-1} s_i = \frac{K}{T}, \quad s_{max} = \max\{s_0, \dots, s_{T-1}\}, \quad \text{and } \theta = \frac{s_{max}}{\bar{s}}.$$

We define

$$h(x) = \left(\sqrt{1 + (e/x)^2} - e/x \right)^2, \quad g(x) = \min \left\{ \frac{1}{ex}, h(x) \right\},$$

and denote by γ the smallest solution satisfying

$$\gamma \geq \frac{2}{1 - \bar{\alpha}} + \frac{2^4 \cdot \bar{\alpha}}{1 - \bar{\alpha}} \left(\frac{\sigma}{(1 - \sqrt{\bar{\alpha}})^2} + \frac{1}{\sigma(1 - \bar{\alpha}) - 2e\sqrt{\bar{\alpha}}\sigma} e^3 \right) e^{3/\sigma^2} \text{ with } \bar{\alpha} = \frac{\epsilon N}{\gamma K}.$$

If the following requirements are satisfied:

$$\bar{s} \leq \frac{g\left(\sqrt{2(\epsilon + \ln(1/\delta))/\epsilon}\right)}{\theta} \cdot N, \tag{9}$$

$$\epsilon \leq \gamma h(\sigma) \cdot \frac{K}{N}, \tag{10}$$

$$\epsilon \geq \gamma \theta^2 \cdot \frac{K}{N} \cdot \frac{\bar{s}}{N}, \text{ and} \tag{11}$$

$$\sigma \geq \sqrt{2(\epsilon + \ln(1/\delta))/\epsilon}, \tag{12}$$

then Algorithm 1 is (ϵ, δ) -differentially private.

Theorems 3 and 2 hold for the more general *asynchronous mini-batch SGD algorithm* (which follows Hogwild!’s philosophy [Recht et al., 2011, De Sa et al., 2015, Zhang et al., 2016, Nguyen et al., 2018, Leblond et al., 2018, van Dijk et al., 2020]) *with DP* in Supplemental Material A. The asynchronous setting allows clients to adapt their sample sizes to their processing speed and communication latency.

We notice that polynomial increasing sample size sequences $s_i \sim qNi^p$ have $\bar{s} \approx [qNT^{p+1}/(p+1)]/T$ and $s_{max} = qNT^p$, hence, $\theta = 1 + p$. This show that our theory covers e.g. linear increasing sample size sequences as discussed in [van Dijk et al., 2020], where is explained how this implies reduced round communication – another metric which one may trade-off against accuracy and total local number K of gradient computations.

Utility σ : In the DP approach, the utility which we wish to achieve measures accuracy. We aim at sufficient high accuracy. We cannot write out this utility function in closed form. In Section 7 we simulate for various σ the accuracy achieved by a global optimal model generated without adding any noise during any of the rounds except for the very last round. This upper bounds the accuracy that can be achieved if noise were added at the end of each round as in DP-SGD. The result is a utility graph which can be used to upper bound σ beyond which the accuracy will certainly suffer too much.

We set σ as large as possible with respect to the accuracy we wish to have. Given this σ we want to max out on our privacy budget. That is, we satisfy (12) with equality, see (6) in the introduction. We discuss (6) with constraints (9), (10), and (11) below:

Neglect (9) and (10): In practice, we need a sufficiently strong DP guarantee, hence, $\delta \leq 1/N$ and ϵ is small enough (preferably smaller than $\epsilon = 0.5$, see Section 5). This means that we will stretch σ to typical values $\sigma = 10, 20$, or 35 such that accuracy will not be compromised too much and at the same time we can achieve sufficient differential privacy. For such σ we have $h(\sigma) \approx 1$ and $g(\sqrt{2(\epsilon + \ln(1/\delta))/\epsilon}) = g(\sigma) = 1/(e\sigma)$ (the first equality follows from (6)). This reduces requirement (9) to $\bar{s} \leq N/(e\sigma\theta)$ and requirement (10) to $\epsilon \leq \gamma K/N$. Notice that (11) in combination with $\epsilon \leq \frac{\gamma\theta}{e\sigma} K/N$ implies condition $\bar{s} \leq N/(e\sigma\theta)$. This implies that (9) and (10) are satisfied for

$$\epsilon \leq \min \left\{ \gamma, \frac{\gamma\theta}{e\sigma} \right\} \cdot \frac{K}{N},$$

which, since $\gamma \geq 2, \theta \geq 1, \sigma$ is in the range of 10, 20, or 35, and K consists of multiple (think 50 or 100s of) epochs (of size N) computation, is generally true for small enough ϵ offering a sufficiently strong DP guarantee. We conclude that (9) and (10) are automatically satisfied in general practical settings (by (11) and small ϵ).

Remaining constraint (11): By using (6), (11) can be equivalently recast as an upper bound on σ ,

$$\sigma \leq \sqrt{\frac{2(\epsilon + \ln(1/\delta))}{\gamma\theta^2 \cdot (K/N) \cdot (\bar{s}/N)}}.$$

Here, γ is a function of σ because γ depends on ϵ in $\bar{\alpha}$ which is a function of σ through (6). However, the definition of γ shows that for small ϵ , γ is close to 2 and this gives $\sqrt{\ln(1/\delta)/(\theta^2 \cdot (K/N) \cdot (\bar{s}/N))}$ as a good approximation of the upper bound. Notice that substituting $\bar{s} = K/T$ yields (7), see Section 5. We conclude that (9, 10, 11, 12) can be replaced by (6, 7) for practical settings. We remind the reader that Section 5 interprets (6, 7), derives the equivalent constraint (8) in place of (7), and explains the benefit of σ ’s independence of T .

Notice that we only argue that (9, 10, 11, 12) can be replaced by (6, 7) for practical settings, however, when designing a parameter setting we still need to verify whether (6, 7) is indeed sufficient. Therefore, the simulations in the next section are based on parameters that satisfy the exact theorem’s constraints (6, 10, 11, 12).

7 Experiments

Our goal is to show that the more general asynchronous differential privacy framework (asynchronous DP-SGD which includes DP-SGD of Algorithm 1) of Supplemental Material A ensures a strong privacy guarantee, i.e, can work with very small ϵ (and $\delta = 1/N$), while having a good convergence rate to good accuracy. We refer to Supplementary Material C for simulation details and complete parameter settings.

Objective function. We summarize experimental results of our asynchronous DP-SGD framework for strongly convex, plain convex and non-convex objective functions with *constant sample size sequences*. As the plain convex objective function we use logistic regression: The weight vector w and bias value b of the logistic function can be learned by minimizing the log-likelihood function J :

$$J = - \sum_{i=1}^N [y_i \cdot \log(\bar{\sigma}_i) + (1 - y_i) \cdot \log(1 - \bar{\sigma}_i)],$$

where N is the number of training samples (x_i, y_i) with $y_i \in \{0, 1\}$, and $\bar{\sigma}_i = 1/(1 + e^{-(w^\top x_i + b)})$ is the sigmoid function. The goal is to learn a vector/model w^* which represents a pair $\bar{w} = (w, b)$ that minimizes J . Function J changes into a strongly convex problem by adding ridge regularization with a regularization parameter $\lambda > 0$, i.e., we minimize $\hat{J} = J + \frac{\lambda}{2} \|\bar{w}\|^2$ instead of J . For simulating non-convex problems, we choose a simple neural network (LeNet) [LeCun et al., 1998] with cross entropy loss function for image classification.

Asynchronous DP-SGD setting. The experiments are conducted with 5 compute nodes and 1 central server. For simplicity, the compute nodes have iid datasets.

7.1 Utility graph

Since we do not have a closed form to describe the relation between the utility of the model (i.e., prediction accuracy) and σ , we propose a heuristic approach to learn the the range of σ from which we may select σ for finding the best (ϵ, δ) -DP. The utility graphs – Figures 1a, 2a and 3a – show the fraction of test accuracy between the model $F(w + n)$ over the original model $F(w)$ (without noise), where $n \sim \mathcal{N}(0, C^2 \sigma^2 \mathbf{I})$ for various values of the clipping constant C and noise standard deviation σ . Intuitively, the closer $F(w + n)/F(w)$ to 1, the better accuracy wrt to $F(w)$. Note that w can be any solution and in the utility graphs, we choose $w = w^*$ with w^* being near to an optimal solution.

The smaller C , the larger σ can be, hence, ϵ can be smaller which gives stronger privacy. However, the smaller C , the more iterations (larger K) are needed for convergence.

In next experiments we use clipping constant $C = 0.1$, which gives a drop of at most 10% in test accuracy for $\sigma \leq 20$ for both strongly convex and plain convex objective functions. To keep the test accuracy loss less or equal to 10% in the non-convex case, we choose $C = 0.025$ and $\sigma \leq 12$.

7.2 Asynchronous DP-SGD with different constant sample size

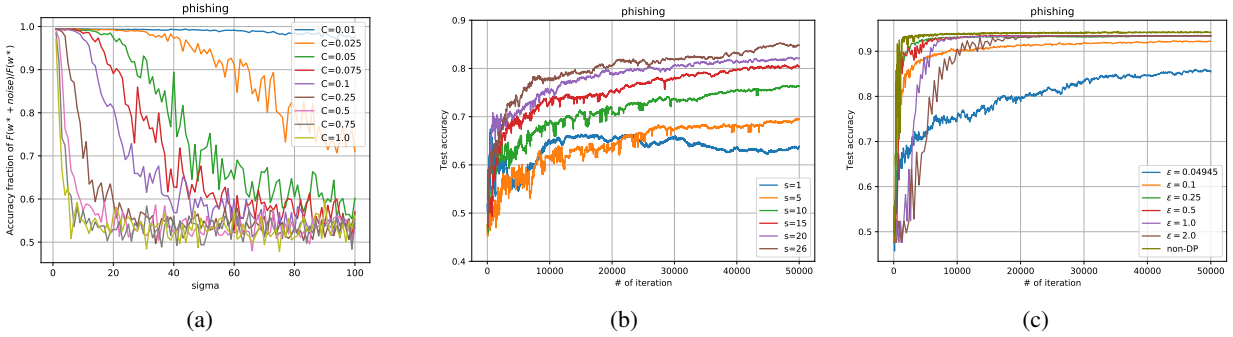


Figure 1: Strongly convex. (a) Utility graph, (b) Different s , (c) Different ϵ

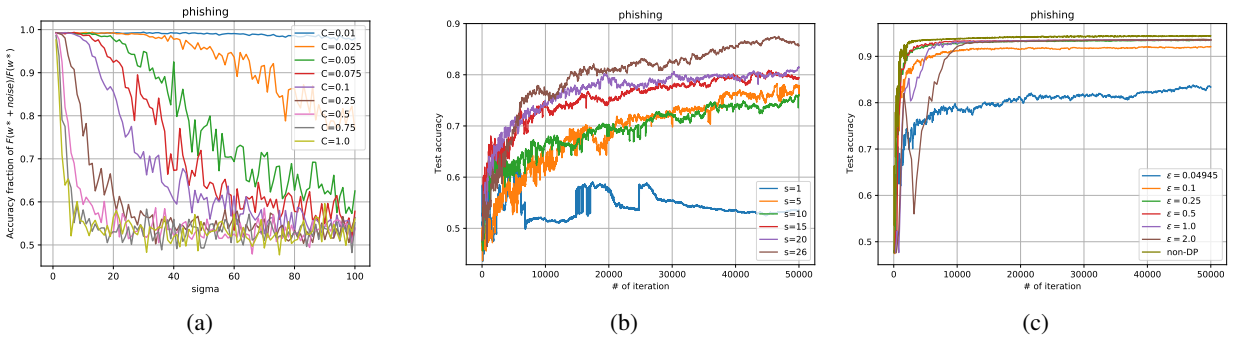


Figure 2: Plain convex. (a) Utility graph, (b) Different s , (c) Different ϵ

Figure 1b and Figure 2b illustrate the test accuracy of our asynchronous DP-SGD with various constant sample sizes for the strongly convex and plain convex cases. Here, we use privacy budget $\epsilon = 0.04945$ and noise $\sigma = 19.2$. It is clear that with $s = 1$, the algorithm shows a bad test accuracy though this constant sample size has the maximum communication rounds. When we use a bigger constant sample size s , for example, $s = 26$, our algorithm can

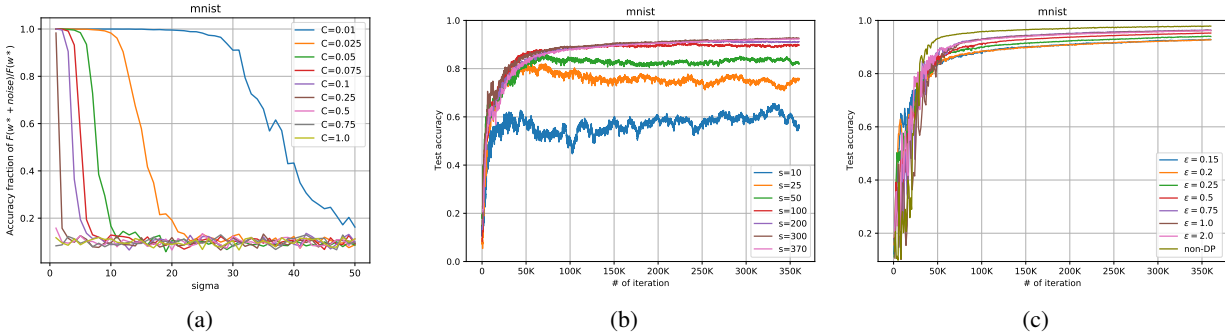


Figure 3: Non-convex. (a) Utility graph, (b) Different s , (c) Different ϵ

achieve the desired performance, when compared to other constant sample sizes. The experiment is extended to the non-convex case as shown in Figure 3b, where we can see a similar pattern. Experimental results for other data sets are in Supplemental Material C. This confirms that our DP-SGD framework can converge to a decent accuracy while achieving a very small privacy budget ϵ .

7.3 Asynchronous DP-SGD with different levels of privacy budget

Figure 1c and Figure 2c show that our DP-SGD framework converges to better accuracy if ϵ is slightly larger. E.g., in the strongly convex case, privacy budget $\epsilon = 0.04945$ achieves test accuracy 86% compared to 93% without differential privacy (hence, no added noise); $\epsilon = 0.1$, still significantly smaller than what is reported in literature, achieves test accuracy 91%. Figure 3c shows the test accuracy of our asynchronous DP-SGD for different privacy budgets ϵ in the non-convex case. For $\epsilon = 0.15$, our framework can achieve the test accuracy about 93%, compared to 98% without differential privacy. These figures again confirm the effectiveness of our DP-SGD framework, which can obtain a strong differential privacy guarantee.

8 Conclusion

We proved a new differential privacy guarantee for DP-SGD which is independent of the total number of communication rounds, attains significantly smaller ϵ than what has been reported in literature, and does this for reasonable DP noise such that test accuracy does not suffer much. This brings DP-SGD to practice.

References

- Martin Abadi, Andy Chu, Ian Goodfellow, H Brendan McMahan, Ilya Mironov, Kunal Talwar, and Li Zhang. Deep learning with differential privacy. In *Proceedings of the 2016 ACM SIGSAC Conference on Computer and Communications Security*, pages 308–318. ACM, 2016.
- Abhishek Bhowmick, John Duchi, Julien Freudiger, Gaurav Kapoor, and Ryan Rogers. Protection against reconstruction and its applications in private federated learning, 2019.
- Chih-Chung Chang and Chih-Jen Lin. LIBSVM: A library for support vector machines. *ACM Transactions on Intelligent Systems and Technology*, 2:27:1–27:27, 2011.
- Christopher M De Sa, Ce Zhang, Kunle Olukotun, and Christopher Ré. Taming the wild: A unified analysis of hogwild-style algorithms. In *NIPS*, pages 2674–2682, 2015.
- John C. Duchi, Michael I. Jordan, and Martin J. Wainwright. Local privacy, data processing inequalities, and statistical minimax rates, 2014.
- Cynthia Dwork. A firm foundation for private data analysis. *Communications of the ACM*, 54(1):86–95, 2011.
- Cynthia Dwork, Krishnaram Kenthapadi, Frank McSherry, Ilya Mironov, and Moni Naor. Our data, ourselves: Privacy via distributed noise generation. In *Annual International Conference on the Theory and Applications of Cryptographic Techniques*, pages 486–503. Springer, 2006a.
- Cynthia Dwork, Frank McSherry, Kobbi Nissim, and Adam Smith. Calibrating noise to sensitivity in private data analysis. In *Theory of cryptography conference*, pages 265–284. Springer, 2006b.
- Cynthia Dwork, Aaron Roth, et al. The algorithmic foundations of differential privacy. *Foundations and Trends® in Theoretical Computer Science*, 9(3–4):211–407, 2014.
- Jonas Geiping, Hartmut Bauermeister, Hannah Dröge, and Michael Moeller. Inverting gradients – how easy is it to break privacy in federated learning?, 2020.
- Robin C. Geyer, Tassilo Klein, and Moin Nabi. Differentially private federated learning: A client level perspective, 2018.
- Meng Hao, Hongwei Li, Xizhao Luo, Guowen Xu, Haomiao Yang, and Sen Liu. Efficient and privacy-enhanced federated learning for industrial artificial intelligence. *IEEE Transactions on Industrial Informatics*, 16(10):6532–6542, 2020. doi: 10.1109/TII.2019.2945367.
- Rémi Leblond, Fabian Pedregosa, and Simon Lacoste-Julien. Improved asynchronous parallel optimization analysis for stochastic incremental methods. *JMLR*, 19(1):3140–3207, 2018.
- Yann LeCun and Corinna Cortes. MNIST handwritten digit database. 2010. URL <http://yann.lecun.com/exdb/mnist/>.
- Yann LeCun, Léon Bottou, Yoshua Bengio, and Patrick Haffner. Gradient-based learning applied to document recognition. *Proceedings of the IEEE*, 86(11):2278–2324, 1998.
- Lingjuan Lyu, Han Yu, and Qiang Yang. Threats to federated learning: A survey, 2020.
- Brendan McMahan, Daniel Ramage, Kunal Talwar, and Li Zhang. Learning differentially private recurrent language models. In *International Conference on Learning Representations (ICLR)*, 2018. URL <https://openreview.net/pdf?id=BJ0hF1Z0b>.
- Mohammad Naseri, Jamie Hayes, and Emiliano De Cristofaro. Toward robustness and privacy in federated learning: Experimenting with local and central differential privacy, 2021.
- M. Nasr, R. Shokri, and A. Houmansadr. Comprehensive privacy analysis of deep learning: Passive and active white-box inference attacks against centralized and federated learning. In *2019 IEEE Symposium on Security and Privacy (SP)*, pages 739–753, 2019. doi: 10.1109/SP.2019.00065.
- Lam M Nguyen, Phuong Ha Nguyen, Marten van Dijk, Peter Richtárik, Katya Scheinberg, and Martin Takáč. Sgd and hogwild! convergence without the bounded gradients assumption. *arXiv preprint arXiv:1802.03801*, 2018.
- Nicolas Papernot, Shuang Song, Ilya Mironov, Ananth Raghunathan, Kunal Talwar, and Úlfar Erlingsson. Scalable private learning with pate, 2018.
- Benjamin Recht, Christopher Re, Stephen Wright, and Feng Niu. Hogwild: A lock-free approach to parallelizing stochastic gradient descent. In *Advances in neural information processing systems*, pages 693–701, 2011.
- Nicolas Le Roux, Mark Schmidt, and Francis Bach. A stochastic gradient method with an exponential convergence rate for finite training sets. *arXiv preprint arXiv:1202.6258*, 2012.

- Reza Shokri, Marco Stronati, Congzheng Song, and Vitaly Shmatikov. Membership inference attacks against machine learning models. In *2017 IEEE Symposium on Security and Privacy (SP)*, pages 3–18. IEEE, 2017.
- L. Song, R. Shokri, and P. Mittal. Membership inference attacks against adversarially robust deep learning models. In *2019 IEEE Security and Privacy Workshops (SPW)*, pages 50–56, 2019. doi: 10.1109/SPW.2019.00021.
- Stacey Truex, Nathalie Baracaldo, Ali Anwar, Thomas Steinke, Heiko Ludwig, Rui Zhang, and Yi Zhou. A hybrid approach to privacy-preserving federated learning, 2019.
- Marten van Dijk, Nhung V Nguyen, Toan N Nguyen, Lam M Nguyen, Quoc Tran-Dinh, and Phuong Ha Nguyen. Hogwild! over distributed local data sets with linearly increasing mini-batch sizes. *arXiv preprint arXiv:2010.14763*, 2020.
- Lei Yu, Ling Liu, Calton Pu, Mehmet Emre Gursoy, and Stacey Truex. Differentially private model publishing for deep learning. *2019 IEEE Symposium on Security and Privacy (SP)*, May 2019. doi: 10.1109/sp.2019.00019. URL <http://dx.doi.org/10.1109/SP.2019.00019>.
- Huan Zhang, Cho-Jui Hsieh, and Venkatesh Akella. Hogwild++: A new mechanism for decentralized asynchronous stochastic gradient descent. In *2016 IEEE 16th International Conference on Data Mining (ICDM)*, pages 629–638. IEEE, 2016.
- Bo Zhao, Konda Reddy Mopuri, and Hakan Bilen. idlg: Improved deep leakage from gradients, 2020.
- Ligeng Zhu, Zhijian Liu, and Song Han. Deep leakage from gradients. *CoRR*, abs/1906.08935, 2019. URL <http://arxiv.org/abs/1906.08935>.

Supplementary Material

A Asynchronous Mini-Batch DP-SGD

Algorithms[†] 2, 3, and 4 explain in pseudo code our asynchronous LDP approach. It is based on the Hogwild! [Recht et al., 2011] recursion

$$w_{t+1} = w_t - \eta_t \nabla f(\hat{w}_t; \xi_t), \quad (13)$$

where \hat{w}_t represents the vector used in computing the gradient $\nabla f(\hat{w}_t; \xi_t)$ and whose vector entries have been read (one by one) from an aggregate of a mix of previous updates that led to w_j , $j \leq t$. In a single-thread setting where updates are done in a fully consistent way, i.e. $\hat{w}_t = w_t$, yields SGD with diminishing step sizes $\{\eta_t\}$.

Recursion (13) models asynchronous SGD. The amount of asynchronous behavior that can be tolerated is given by some function $\tau(t)$, see [Nguyen et al., 2018] where this is analysed for strongly convex objective functions: We say that the sequence $\{w_t\}$ is consistent with delay function τ if, for all t , vector \hat{w}_t includes the aggregate of the updates up to and including those made during the $(t - \tau(t))$ -th iteration, i.e.,

$$\hat{w}_t = w_0 - \sum_{j \in \mathcal{U}} \eta_j \nabla f(\hat{w}_j; \xi_j)$$

for some \mathcal{U} with $\{0, 1, \dots, t - \tau(t) - 1\} \subseteq \mathcal{U}$.

In Algorithm 4 the local SGD iterations all compute gradients based on the same local model \hat{w} , which gets substituted by a newer global model \hat{v}_k as soon as it is received by the interrupt service routine `ISRRECEIVE`. As explained in `ISRRECEIVE` \hat{v}_k includes all the updates from all the clients up to and including their local rounds $\leq k$. This shows that locally the delay τ can be estimated based on the current local round i together with k . Depending on how much delay can be tolerated `SETUP` defines $\Upsilon(k, i)$ to indicate whether the combination (k, i) is permissible (i.e., the corresponding delay aka asynchronous behavior can be tolerated). It has been shown that for strongly convex objective functions (without DP enhancement) the convergence rate remains optimal even if the delay $\tau(t)$ is as large as $\approx \sqrt{t/\ln t}$ [Nguyen et al., 2018]. Similar behavior has been reported for plain convex and non-convex objective functions in [van Dijk et al., 2020].

In Algorithm 4 we assume that messages/packets never drop; they will be resent but can arrive out of order. This guarantees that we get out of the "while $\Upsilon(k, i)$ is false loop" because at some moment the server receives all the updates in order to broadcast a new global model \hat{v}_{k+1} and once received by `ISRRECEIVE` this will increment k and make $\Upsilon(k, i)$ true which allows `LOCALSGDWITHDP` to exit the wait loop. As soon as the wait loop is exited we know that all local gradient computations occur when $\Upsilon(k, i)$ is true which reflect that these gradient computations correspond to delays that are permissible (in that we still expect convergence of the global model to good accuracy).

Algorithm 2 Client – Local model with Differential Privacy

1: **procedure** `SETUP`(n):

Initialize sample size sequence $\{s_i\}_{i=0}^T$, (diminishing) round step sizes $\{\bar{\eta}_i\}_{i=0}^T$, and a default global model \hat{v}_0 to start with.

Define a permissible delay function $\Upsilon(k, i) \in \{\mathbf{True}, \mathbf{False}\}$ which takes the current local round number i and the round number k of the last received global model into account to find out whether local SGD should wait till a more recent global model is received. $\Upsilon(\cdot, \cdot)$ can also make use of knowledge of the sample size sequences used by each of the clients.

2: **end procedure**

In this paper we analyse the Gaussian based differential privacy method of [Abadi et al., 2016]. We use their clipping method; rather than using the gradient $\nabla f(\hat{w}, \xi)$ itself, we use its clipped version $[\nabla f(\hat{w}, \xi)]_C$ where $[x]_C = x / \max\{1, \|x\|/C\}$. Also, we use the same mini-batch approach where before the start of the i -th local round

[†]Our pseudocode uses the format from [van Dijk et al., 2020].

Algorithm 3 Client – Local model with Differential Privacy

1: **procedure** ISRRECEIVE(\hat{v}_k):

This Interrupt Service Routine is called whenever a new broadcast global model \hat{v}_k is received from the server. Once received, *the client's local model \hat{w} is replaced with \hat{v}_k (if no more recent global model $\hat{v}_{>k}$ was received out of order before receiving this \hat{v}_k)*

The server broadcasts global model \hat{v}_k for global round number k once the updates corresponding to local round numbers $\leq k - 1$ from *all* clients have been received and have been aggregated into the global model. The server aggregates updates from clients into the current global model as soon as they come in. This means that \hat{v}_k includes all the updates from all the clients up to and including their local round numbers $\leq k - 1$ and potentially includes updates corresponding to later round numbers from subsets of clients. The server broadcasts the global round number k together with \hat{v}_k .

2: **end procedure**

Algorithm 4 Client – Local model with Differential Privacy

1: **procedure** LOCALSGDWITHDP(d)

2: $i = 0, \hat{w} = \hat{v}_0$

3: **while** True **do**

4: **while** $\Upsilon(k, i) = \text{False}$ **do** nothing **end**

5: Uniformly sample a random set $\{\xi_h\}_{h=1}^{s_i} \subseteq d$

6: $h = 0, U = 0$

7: **while** $h < s_i$ **do**

8: $g = [\nabla f(\hat{w}, \xi_h)]_C$

9: $U = U + g$

10: $h++$

11: **end while**

12: $n \leftarrow \mathcal{N}(0, C^2 \sigma_i^2 \mathbf{I})$

13: $U = U + n$

14: $\hat{w} = \hat{w} + \bar{\eta}_i \cdot U$

15: Send (i, U) to the Server.

16: $i++$

17: **end while**

18: **end procedure**

a random min-batch of sample size s_i is selected. During the inner loop the sum of gradient updates is maintained where each of the gradients correspond to the same local model \hat{w} until it is replaced by a newer global model. In supplementary material B we show that this is needed for proving DP guarantees and that generalizing the algorithm by locally implementing the Hogwild! recursion itself (which updates the local model each iteration) does not work together with the DP analysis. So, our approach only uses the Hogwild! concept at a global round by round interaction level.

At the end of each local round the sum of updates U is obfuscated with Gaussian noise; Gaussian noise $\mathcal{N}(0, C^2 \sigma_i^2)$ is added to each vector entry. In this general description σ_i is round dependent, but our DP analysis in Supplementary Material B must from some point onward assume a constant $\sigma = \sigma_i$ over all rounds. The noised U times the round step size $\bar{\eta}_i$ is added to the local model after which a new local round starts again.

The noised U is also transmitted to the server who adds U times the round step size $\bar{\eta}_i$ to its global model \hat{v} . As soon as all clients have submitted their updates up to and including their local rounds $\leq k - 1$, the global model \hat{v} , denoted as \hat{v}_k , is broadcast to all clients, who in turn replace their local models with the newly received global model. Notice that \hat{v}_k may include updates from a subset of client that correspond to local rounds $\geq k$.

The presented algorithm adapts to asynchronous behavior in the following two ways: We explained above that the broadcast global models \hat{v}_k themselves include a mix of received updates that correspond to local rounds $\geq k$ – this is due to asynchronous behavior. Second, the sample size sequence $\{s_i\}$ does not necessarily need to be fixed a-priori during SETUP (the round step size sequence $\{\bar{\eta}_i\}$ does need to be fixed a-priori). In fact, the client can adapt its sample sizes s_i on the fly to match its speed of computation and communication latency. This allows the client to adapt its local mini-batch SGD to its asynchronous behavior due to the scheduling of its own resources. Our DP analysis holds for a wide range of varying sample size sequences.

We notice that adapting sample size sequences on a per client basis still fits the same overall objective function as long as all local data sets are iid: This is because iid implies that the execution of the presented algorithm can be cast in a single Hogwild! recursion where the ξ_h are uniformly chosen from a common data source distribution \mathcal{D} . This corresponds to the stochastic optimization problem

$$\min_{w \in \mathbb{R}^d} \{F(w) = \mathbb{E}_{\xi \sim \mathcal{D}}[f(w; \xi)]\},$$

which defines objective function F (independent of the locally used sample size sequences). Local data sets being iid in the sense that they are all, for example, drawn from car, train, boat, etc images benefit from DP in that car details (such as an identifying number plate), boat details, etc. need to remain private.

B Differential privacy proofs

In order to prove Theorem 2, we first set up the differential privacy framework of [Abadi et al., 2016] in Supplemental Material B.1. Here we enhance a core lemma by proving a concrete bound rather than an asymptotic bound on the so-called λ -th moment which plays a crucial role in the differential privacy analysis. The concrete bound makes explicit the higher order error term in [Abadi et al., 2016].

Next in Supplemental Material B.2 we generalize Theorem 1 [Abadi et al., 2016]:

Theorem 3. *We assume that $\sigma = \sigma_i$ with $\sigma \geq 216/215$. for all rounds i . Let*

$$r = r_0 \cdot 2^3 \cdot \left(\frac{1}{1 - u_0} + \frac{1}{1 - u_1} \frac{e^3}{\sigma^3} \right) e^{3/\sigma^2} \text{ with } u_0 = \frac{2\sqrt{r_0\sigma}}{\sigma - r_0} \text{ and } u_1 = \frac{2e\sqrt{r_0\sigma}}{(\sigma - r_0)\sigma},$$

where r_0 is such that it satisfies

$$r_0 \leq 1/e, \quad u_0 < 1, \quad \text{and } u_1 < 1.$$

Let the sample size sequence satisfy $s_i/N \leq r_0/\sigma$. For $j = 1, 2, 3$ we define \hat{S}_j (resembling an average over the sum of j -th powers of s_i/N) with related constants ρ and $\hat{\rho}$:

$$\hat{S}_j = \frac{1}{T} \sum_{i=0}^{T-1} \frac{s_i^j}{N(N - s_i)^{j-1}}, \quad \frac{\hat{S}_1 \hat{S}_3}{\hat{S}_2^2} \leq \rho \text{ and } \frac{\hat{S}_1^2}{\hat{S}_2} \leq \hat{\rho}.$$

Let $\epsilon = c_1 T \hat{S}_1^2$. Then, Algorithm 4 is (ϵ, δ) -differentially private if

$$\sigma \geq \frac{2}{\sqrt{c_0}} \frac{\sqrt{\hat{S}_2 T (\epsilon + \ln(1/\delta))}}{\epsilon} \text{ where } c_0 = c(c_1) \text{ with } c(x) = \min \left\{ \frac{\sqrt{2r\rho x + 1} - 1}{r\rho x}, \frac{2}{\hat{\rho}x} \right\}.$$

This generalizes Theorem 1 where all $s_i = s$ are constant. First, Theorem 3 covers a much broader class of sample size sequences that satisfy bounds on their 'moments' \hat{S}_j (this is more clear as a consequence of Theorem 3). Second, our detailed analysis provides a tighter bound in that it makes the relation between "constants" c_0 and c_1 explicit, contrary to [Abadi et al., 2016]. Exactly due to this relation $c_0 = c(c_1)$ we are able to prove in Supplemental Material B.3 Theorem 2 as a consequence of Theorem 3 by considering the case $c(c_1) = 2/(\hat{\rho}c_1)$.

B.1 Definitions

We base our proofs on the framework and theory presented in [Abadi et al., 2016]. In order to be on the same page we repeat and cite word for word their definitions:

For neighboring databases d and d' , a mechanism \mathcal{M} , auxiliary input aux , and an outcome o , define the privacy loss at o as

$$c(o; \mathcal{M}, \text{aux}, d, d') = \ln \frac{\Pr[\mathcal{M}(\text{aux}, d) = o]}{\Pr[\mathcal{M}(\text{aux}, d') = o]}.$$

For a given mechanism \mathcal{M} , we define the λ -th moment $\alpha_{\mathcal{M}}(\lambda; \text{aux}, d, d')$ as the log of the moment generating function evaluated at the value λ :

$$\alpha_{\mathcal{M}}(\lambda; \text{aux}, d, d') = \ln \mathbf{E}_{o \sim \mathcal{M}(\text{aux}, d)}[\exp(\lambda \cdot c(o; \mathcal{M}, \text{aux}, d, d'))].$$

We define

$$\alpha_{\mathcal{M}}(\lambda) = \max_{\mathbf{aux}, d, d'} \alpha_{\mathcal{M}}(\lambda; \mathbf{aux}, d, d')$$

where the maximum is taken over all possible \mathbf{aux} and all the neighboring databases d and d' .

We first take Lemma 3 from [Abadi et al., 2016] and make explicit their order term $O(q^3 \lambda^3 / \sigma^3)$ with $q = s_{i,c}$ and $\sigma = \sigma_i$ in our notation. The lemma considers as mechanism \mathcal{M} the i -th round of gradient updates and we abbreviate $\alpha_{\mathcal{M}}(\lambda)$ by $\alpha_i(\lambda)$. The auxiliary input of the mechanism at round i includes all the output of the mechanisms of previous rounds (as in [Abadi et al., 2016]).

For the local mini-batch SGD the mechanism \mathcal{M} of the i -th round is given by

$$\mathcal{M}(\mathbf{aux}, d) = \sum_{h=0}^{s_i-1} [\nabla f(\hat{w}, \xi_h)]_C + \mathcal{N}(0, C^2 \sigma_i^2 \mathbf{I}),$$

where \hat{w} is the local model at the start of round i which is replaced by a new global model \hat{w} as soon as a new \hat{w} is received from the server (see ISRRReceive), and where ξ_h are drawn from training data d , and $[\cdot]_C$ denotes clipping (that is $[x]_C = x / \max\{1, \|x\|_2/C\}$). In order for \mathcal{M} to be able to compute its output, it needs to know the global models received in round i and it needs to know the starting local model \hat{w} . To make sure \mathcal{M} has all this information, \mathbf{aux} represents the collection of all outputs generated by the mechanisms of previous rounds $< i$ together with the global models received in round i itself.

In the next subsection we will use the framework of [Abadi et al., 2016] and apply its composition theory to derive bounds on the privacy budget (ϵ, δ) for the whole computation consisting of T rounds that reveal the outputs of the mechanisms for these T rounds as described above.

We remind the reader that s_i/N is the probability of selecting a sample from a sample set (batch) of size s_i out of a training data set d' of size $N = |d'|$; σ_i corresponds to the $\mathcal{N}(0, C^2 \sigma_i^2 \mathbf{I})$ noise added to the mini-batch gradient computation in round i (see the mechanism described above).

Lemma 1. *Assume a constant $r_0 < 1$ and deviation $\sigma_i \geq 216/215$ such that $s_i/N \leq r_0/\sigma_i$. Suppose that λ is a positive integer with*

$$\lambda \leq \sigma_i^2 \ln \frac{N}{s_i \sigma_i}$$

and define

$$U_0(\lambda) = \frac{2\sqrt{\lambda r_0/\sigma_i}}{\sigma_i - r_0} \text{ and } U_1(\lambda) = \frac{2e\sqrt{\lambda r_0/\sigma_i}}{(\sigma_i - r_0)\sigma_i}.$$

Suppose $U_0(\lambda) \leq u_0 < 1$ and $U_1(\lambda) \leq u_1 < 1$ for some constants u_0 and u_1 . Define

$$r = r_0 \cdot 2^3 \left(\frac{1}{1 - u_0} + \frac{1}{1 - u_1} \frac{e^3}{\sigma_i^3} \right) \exp(3/\sigma_i^2).$$

Then,

$$\alpha_i(\lambda) \leq \frac{s_i^2 \lambda (\lambda + 1)}{N(N - s_i) \sigma_i^2} + \frac{r}{r_0} \cdot \frac{s_i^3 \lambda^2 (\lambda + 1)}{N(N - s_i)^2 \sigma_i^3}.$$

Proof. The start of the proof of Lemma 3 in [Abadi et al., 2016] implicitly uses the proof of Theorem A.1 in [Dwork et al., 2014], which up to formula (A.2) shows how the 1-dimensional case translates into a privacy loss that corresponds to the 1-dimensional problem defined by μ_0 and μ_1 in the proof of Lemma 3 in [Abadi et al., 2016], and which shows at the end of the proof of Theorem A.1 (p. 268 [Dwork et al., 2014]) how the multi-dimensional problem transforms into the 1-dimensional problem. In the notation of Theorem A.1, $f(D) + \mathcal{N}(0, \sigma^2 \mathbf{I})$ represents the general (random) mechanism $\mathcal{M}(D)$, which for Lemma 3 in [Abadi et al., 2016]'s notation should be interpreted as the batch computation

$$\mathcal{M}(d) = \sum_{h \in J} f(d_h) + \mathcal{N}(0, \sigma^2 \mathbf{I})$$

for a random sample/batch $\{d_h\}_{h \in J}$. Here, $f(d_h)$ (by abuse of notation – in this context f does not represent the objective function) represent clipped gradient computations $\nabla f(\hat{w}; d_h)$ where \hat{w} is the last received global model with which round i starts (Lemma 3 in [Abadi et al., 2016] uses clipping constant $C = 1$, hence $\mathcal{N}(0, C^2 \sigma^2 \mathbf{I}) = \mathcal{N}(0, \sigma^2 \mathbf{I})$).

Let us detail the argument of the proof of Lemma 3 in [Abadi et al., 2016] in order to understand what flexibility is possible: We consider two data sets $d = \{d_1, \dots, d_{N-1}\}$ and $d' = d + \{d_N\}$, where $d_N \notin d$ represents a new data base element so that d and d' differ in exactly one element. The size of d' is equal to N . We define vector x as the sum

$$x = \sum_{J \setminus \{N\}} f(d_i).$$

Let

$$z = f(d_N).$$

If we consider data set d , then sample set $J \subseteq \{1, \dots, N-1\}$ and mechanism $\mathcal{M}(d)$ returns

$$\mathcal{M}(d) = \sum_{h \in J} f(d_h) + \mathcal{N}(0, \sigma^2 \mathbf{I}) = \sum_{h \in J \setminus \{N\}} f(d_h) + \mathcal{N}(0, \sigma^2 \mathbf{I}) = x + \mathcal{N}(0, \sigma^2 \mathbf{I}).$$

If we consider data set d' , then $J \subseteq \{1, \dots, N\}$ contains d_N with probability $q = |J|/N$ ($|J| = s_i$ is the sample size used in round i). In this case mechanism $\mathcal{M}(d')$ returns

$$\mathcal{M}(d') = \sum_{h \in J} f(d_h) + \mathcal{N}(0, \sigma^2 \mathbf{I}) = f(d_N) + \sum_{h \in J \setminus \{N\}} f(d_h) + \mathcal{N}(0, \sigma^2 \mathbf{I}) = z + x + \mathcal{N}(0, \sigma^2 \mathbf{I})$$

with probability q . It returns

$$\mathcal{M}(d') = \sum_{h \in J} f(d_h) + \mathcal{N}(0, \sigma^2 \mathbf{I}) = \sum_{h \in J \setminus \{N\}} f(d_h) + \mathcal{N}(0, \sigma^2 \mathbf{I}) = x + \mathcal{N}(0, \sigma^2 \mathbf{I})$$

with probability $1 - q$. Combining both cases shows that $\mathcal{M}(d')$ represents a mixture of two Gaussian distributions (shifted over a vector x):

$$\mathcal{M}(d') = x + (1 - q) \cdot \mathcal{N}(0, \sigma^2 \mathbf{I}) + q \cdot \mathcal{N}(z, \sigma^2 \mathbf{I}).$$

This high dimensional problem is transformed into a single dimensional problem at the end of the proof of Theorem A.1 (p. 268 [Dwork et al., 2014]) by considering the one dimensional line from point x into the direction of z , i.e., the line through points x and $x + z$; the one dimensional line maps x to the origin 0 and $x + z$ to $\|z\|_2$. $\mathcal{M}(d)$ as well as $\mathcal{M}(d')$ projected on this line are distributed as

$$\mathcal{M}(d) \sim \mu_0 \text{ and } \mathcal{M}(d') \sim (1 - q)\mu_0 + q\mu_1,$$

where

$$\mu_0 \sim \mathcal{N}(0, \sigma^2) \text{ and } \mu_1 \sim \mathcal{N}(\|z\|_2, \sigma^2).$$

In [Abadi et al., 2016] as well as in this paper the gradients are clipped (their Lemma 3 uses clipping constant $C = 1$) and this implies

$$\|z\|_2 = \|f(d_N)\|_2 \leq C = 1.$$

Their analysis continues by assuming the worst-case in differential privacy, that is,

$$\mu_1 \sim \mathcal{N}(1, \sigma^2).$$

Notice that the above argument analyses a local mini-batch SGD computation. Rather than using a local mini-batch SGD computation, can we use clipped SGD iterations which continuously update the local model:

$$\hat{w}_{h+1} = \hat{w}_h - \eta_h \nabla [f(\hat{w}_h, \xi_h)]_C.$$

This should lead to faster convergence to good accuracy compared to a local minibatch computation. However, the above arguments cannot proceed[‡] because (in the notation used above where the $d_h, h \in J$, are the $\xi_h, h \in \{0, \dots, s_i - 1 = |J| - 1\}$) selecting sample d_N in iteration h does not only influence the update computed in iteration h but also influences all iterations after h till the end of the round (because $f(d_N)$ updates the local model in iteration h which is used in the iterations that come after). Hence, the dependency on d_N is directly felt by $f(d_N)$ in iteration h and indirectly felt in the $f(d_j)$ that are computed after iteration h . This means that we cannot represent distribution $\mathcal{M}(d')$ as a clean mix of Gaussian distributions with a mean z , whose norm is bounded by the clipping constant.

The freedom which we do have is replacing the local model by a newly received global model. This is because the updates $f(d_h), h \in J$, computed locally in round i have not yet been transmitted to the server and, hence, have not been

[‡]Unless we assume a general upper bound on the norm of the Hessian of the objective function which should be large enough to cover a wide class of objective functions and small enough in order to be able to derive practical differential privacy guarantees.

aggregated into the global model that was received. In a way the mechanism $\mathcal{M}(d)$ is composed of two (or multiple if more newer and newer global models are received during the round) sums

$$\mathcal{M}(d) = \sum_{h \in J_0} f_0(d_h) + \sum_{h \in J_1} f_1(d_h) + \mathcal{N}(0, \sigma^2 \mathbf{I}),$$

where $J = J_0 \cup J_1$ and J_0 represent local gradient computations, shown by $f_0(\cdot)$, based on the initial local model \hat{w} and J_1 represent the local gradient computations, shown by $f_1(\cdot)$, based on the newly received global model \hat{v} which replaces \hat{w} . As one can verify, the above arguments are still valid for this slight adaptation. As in Lemma 3 in [Abadi et al., 2016] we can now translate our privacy loss to the 1-dimensional problem defined by $\mu_0 \sim \mathcal{N}(0, C^2 \sigma^2)$ and $\mu_1 \sim \mathcal{N}(C, C^2 \sigma^2)$ for $\|\nabla f(\cdot, \cdot)\|_2 \leq C$ as in the proof of Lemma 3 (which after normalization with respect to C gives the formulation of Lemma 3 in [Abadi et al., 2016] for $C = 1$).

The remainder of the proof of Lemma 3 analyses μ_0 and the mix $\mu = (1 - q)\mu_0 + q\mu_1$ leading to bounds for the expectations (3) and (4) in [Abadi et al., 2016] which only depend on μ_0 and μ_1 . Here, q is the probability of having a special data sample ξ (written as d_N in the arguments above) in the batch. In our algorithm $q = s_i/N$. So, we may adopt the statement of Lemma 3 and conclude for the i -th batch computation

$$\alpha_i(\lambda) \leq \frac{s_i^2 \lambda (\lambda + 1)}{N(N - s_i) \sigma_i^2} + O\left(\frac{s_i^3 \lambda^3}{N^3 \sigma_i^3}\right).$$

In order to find an exact expression for the higher order term we look into the details of Lemma 3 of [Abadi et al., 2016]. It computes an upper bound for the binomial tail

$$\sum_{t=3}^{\lambda+1} \binom{\lambda+1}{t} \mathbb{E}_{z \sim \nu_1} [((\nu_0(z) - \nu_1(z))/\nu_1(z))^t], \quad (14)$$

where

$$\begin{aligned} & \mathbb{E}_{z \sim \nu_1} [((\nu_0(z) - \nu_1(z))/\nu_1(z))^t] \\ & \leq \frac{(2q)^t (t-1)!!}{2(1-q)^{t-1} \sigma^t} + \frac{q^t}{(1-q)^t \sigma^{2t}} + \frac{(2q)^t \exp((t^2 - t)/(2\sigma^2)) (\sigma^t (t-1)!! + t^t)}{2(1-q)^{t-1} \sigma^{2t}} \\ & = \frac{(2q)^t (t-1)!! (1 + \exp((t^2 - t)/(2\sigma^2)))}{2(1-q)^{t-1} \sigma^t} + \frac{q^t (1 + (1-q) 2^t \exp((t^2 - t)/(2\sigma^2)) t^t)}{2(1-q)^t \sigma^{2t}} \end{aligned} \quad (15)$$

Since $t \geq 3$, we have the coarse upper bounds

$$1 \leq \frac{\exp((t^2 - t)/(2\sigma^2))}{\exp((3^2 - 3)/(2\sigma^2))} \text{ and } 1 \leq \frac{(1-q) 2^t \exp((t^2 - t)/(2\sigma^2)) t^t}{(1-q) 2^3 \exp((3^2 - 3)/(2\sigma^2)) 3^3}.$$

By defining c as 1 plus the maximum of these two bounds,

$$c = 1 + \frac{\max\{1, 1/((1-q) \cdot 216)\}}{\exp(3/\sigma^2)},$$

we have (15) at most

$$\leq \frac{(2q)^t (t-1)!! c \exp((t^2 - t)/(2\sigma^2))}{2(1-q)^{t-1} \sigma^t} + \frac{q^t c (1-q) 2^t \exp((t^2 - t)/(2\sigma^2)) t^t}{2(1-q)^t \sigma^{2t}}. \quad (16)$$

Generally (for practical parameter settings as we will find out), $q \leq 1 - 1/216$ which makes $c \leq 2$. In the remainder of this proof, we use $c = 2$ and assume $q \leq 215/216$. In fact, assume in the statement of the lemma that $\sigma = \sigma_i \geq 216/215$ which together with $q = s_i/N \leq r_0/\sigma_i$ and $r_0 < 1$ implies $q \leq 215/216$.

After multiplying (16) with the upper bound for

$$\binom{\lambda+1}{t} \leq \frac{\lambda+1}{\lambda} \frac{\lambda^t}{t!}$$

and noticing that $(t-1)!!/t! \leq 1$ and $t^t/t! \leq e^t$ we get the addition of the following two terms

$$\frac{\lambda+1}{\lambda} \frac{\lambda^t (2q)^t \exp((t^2 - t)/(2\sigma^2))}{(1-q)^{t-1} \sigma^t} + \frac{\lambda+1}{\lambda} \frac{\lambda^t q^t (1-q) 2^t \exp((t^2 - t)/(2\sigma^2)) e^t}{(1-q)^t \sigma^{2t}}.$$

This is equal to

$$(1-q) \frac{\lambda+1}{\lambda} \left(\frac{\lambda 2q \exp((t-1)/(2\sigma^2))}{(1-q)\sigma} \right)^t + (1-q) \frac{\lambda+1}{\lambda} \left(\frac{\lambda q 2 \exp(1+(t-1)/(2\sigma^2))}{(1-q)\sigma^2} \right)^t. \quad (17)$$

We notice that by using $t \leq \lambda+1$, $\lambda/\sigma^2 \leq \ln(1/(q\sigma))$ (assumption), and $q = s_{i,c}/N_c \leq r_0/\sigma$ we obtain

$$\frac{\lambda 2q \exp((t-1)/(2\sigma^2))}{(1-q)\sigma} \leq \frac{\lambda 2q \exp(\lambda/(2\sigma^2))}{(1-q)\sigma} \leq \frac{2\sqrt{\lambda q}}{(1-q)\sigma} = \frac{2\sqrt{\lambda r_0/\sigma}}{\sigma - r_0} = U_0(\lambda)$$

and

$$\frac{\lambda q 2 \exp(1+(t-1)/(2\sigma^2))}{(1-q)\sigma^2} \leq \frac{\lambda q 2e \exp(\lambda/(2\sigma^2))}{(1-q)\sigma^2} \leq \frac{2e\sqrt{\lambda q}}{(1-q)\sigma^2} = \frac{2e\sqrt{\lambda r_0/\sigma}}{(\sigma - r_0)\sigma} = U_1(\lambda).$$

Together with our assumption on $U_0(\lambda)$ and $U_1(\lambda)$, this means that the binomial tail (14) is upper bounded by the two terms in (17) after substituting $t = 3$, with the two terms multiplied by

$$\sum_{j=0}^{\infty} U_0(\lambda)^j = \frac{1}{1-U_0(\lambda)} \leq \frac{1}{1-u_0} \quad \text{and} \quad \sum_{j=0}^{\infty} U_1(\lambda)^j = \frac{1}{1-U_1(\lambda)} \leq \frac{1}{1-u_1}$$

respectively. For (14) this yields the upper bound

$$\begin{aligned} & \frac{1}{1-u_0} (1-q) \frac{\lambda+1}{\lambda} \left(\frac{\lambda 2q \exp(1/\sigma^2)}{(1-q)\sigma} \right)^3 + \frac{1}{1-u_1} (1-q) \frac{\lambda+1}{\lambda} \left(\frac{\lambda q 2 \exp(1+1/\sigma^2)}{(1-q)\sigma^2} \right)^3 \\ & \leq \left(\frac{1}{1-u_0} 2^3 \exp(3/\sigma^2) + \frac{1}{1-u_1} \frac{2^3 \exp(3+3/\sigma^2)}{\sigma^3} \right) \cdot \frac{\lambda^2(\lambda+1)q^3}{(1-q)^2\sigma^3}. \end{aligned}$$

By the definition of r , we obtain the bound

$$\leq \frac{r}{r_0} \cdot \frac{\lambda^2(1+\lambda)q^3}{(1-q)^2\sigma^3},$$

which finalizes the proof.

B.2 Proof of Theorem 3

The proof Theorem 3 follows the line of thinking in the proof of Theorem 1 in [Abadi et al., 2016]. Our theorem applies to varying sample/batch sizes and for this reason introduces moments \hat{S}_j . Our theorem explicitly defines the constant used in the lower bound of σ – this is important for proving our second (main) theorem in the next subsection.

Theorem 3 assumes $\sigma = \sigma_i$ for all rounds i with $\sigma \geq 216/215$; constant $r_0 \leq 1/e$ such that $s_i/N \leq r_0/\sigma$; constant

$$r = r_0 \cdot 2^3 \left(\frac{1}{1-u_0} + \frac{1}{1-u_1} \frac{e^3}{\sigma^3} \right) \exp(3/\sigma^2), \quad (18)$$

where

$$u_0 = \frac{2\sqrt{r_0\sigma}}{\sigma - r_0} \quad \text{and} \quad u_1 = \frac{2e\sqrt{r_0\sigma}}{(\sigma - r_0)\sigma}$$

are both assumed < 1 .

For $j = 1, 2, 3$ we define[§]

$$\hat{S}_j = \frac{1}{T} \sum_{i=0}^{T-1} \frac{s_i^j}{N(N-s_i)^{j-1}} \quad \text{with} \quad \frac{\hat{S}_1 \hat{S}_3}{\hat{S}_2^2} \leq \rho, \quad \frac{\hat{S}_1^2}{\hat{S}_2} \leq \hat{\rho}.$$

Based on these constants we define

$$c(x) = \min \left\{ \frac{\sqrt{2r\rho x + 1} - 1}{r\rho x}, \frac{2}{\hat{\rho}x} \right\}.$$

[§] s_i^j denotes the j -th power $(s_i)^j$.

Let $\epsilon = c_1 T \hat{S}_1^2$. We want to prove Algorithm 4 is (ϵ, δ) -differentially private if

$$\sigma \geq \frac{2}{\sqrt{c_0}} \frac{\sqrt{\hat{S}_2 T (\epsilon + \ln(1/\delta))}}{\epsilon} \approx \frac{2}{\sqrt{c_0}} \frac{\sqrt{\hat{S}_2 T \ln(1/\delta)}}{\epsilon} \text{ where } c_0 = c(c_1)$$

(the approximation holds for small ϵ which is what we aim for in this paper).

Proof. For $j = 1, 2, 3$, we define

$$S_j = \sum_{i=0}^{T-1} \frac{s_i^j}{N(N-s_i)^{j-1} \sigma_i^j} \text{ and } S'_j = \frac{1}{T} \sum_{i=0}^{T-1} \frac{s_i^j \sigma_i^j}{N(N-s_i)^{j-1}}.$$

(Notice that $S'_1 \leq r_0$.) Translating Lemma 1 in this notation yields (we will verify the requirement/assumptions of Lemma 1 on the fly below)

$$\sum_{i=0}^{T-1} \alpha_i(\lambda) \leq S_2 \lambda(\lambda + 1) + \frac{r}{r_0} S_3 \lambda^2(\lambda + 1).$$

The composition Theorem 2 in [Abadi et al., 2016] shows that our algorithm for client c is (ϵ, δ) -differentially private for

$$\delta \geq \min_{\lambda} \exp \left(\sum_{i=0}^{T-1} \alpha_i(\lambda) - \lambda \epsilon \right),$$

where T indicates the total number of batch computations and the minimum is over positive integers λ . Similar to their proof we choose λ such that

$$S_2 \lambda(\lambda + 1) + \frac{r}{r_0} S_3 \lambda^2(\lambda + 1) - \lambda \epsilon \leq -\lambda \epsilon / 2. \quad (19)$$

This implies that we can choose δ as small as $\exp(-\lambda \epsilon / 2)$, i.e., if

$$\delta \geq \exp(-\lambda \epsilon / 2), \quad (20)$$

then we have (ϵ, δ) -differential privacy. After dividing by the positive integer λ , inequality (19) is equivalent to the inequality

$$S_2(\lambda + 1) + \frac{r}{r_0} S_3 \lambda(1 + \lambda) \leq \epsilon / 2,$$

which is equivalent to

$$(\lambda + 1) \left(1 + \frac{r}{r_0} \frac{S_3}{S_2} \lambda \right) \leq \frac{\epsilon}{2S_2}.$$

This is in turn implied by

$$\lambda + 1 \leq c_0 \frac{\epsilon}{2S_2} \quad (21)$$

together with

$$c_0 \frac{\epsilon}{2S_2} \left(1 + \frac{r}{r_0} \frac{S_3}{S_2} c_0 \frac{\epsilon}{2S_2} \right) \leq \frac{\epsilon}{2S_2},$$

or equivalently,

$$c_0 \left(1 + \frac{r}{2r_0} \cdot c_0 \cdot \frac{S_3}{S_2^2} \epsilon \right) \leq 1. \quad (22)$$

We use

$$\epsilon = c_1 \cdot T \hat{S}_1^2 = c_1 \cdot S_1 S'_1 \quad (23)$$

(for constant $\sigma_i = \sigma$). This translates our requirements (21) and (22) into

$$\lambda + 1 \leq \frac{c_0 c_1}{2} \frac{S_1 S'_1}{S_2} \text{ and} \quad (24)$$

$$c_0 \left(1 + \frac{r}{2r_0} \cdot c_0 c_1 \frac{S_1 S_3}{S_2^2} S'_1 \right) \leq 1. \quad (25)$$

Since we assume

$$\frac{S_1 S_3}{S_2^2} = \frac{\hat{S}_1 \hat{S}_3}{\hat{S}_2^2} \leq \rho$$

and since we know that $S'_1 \leq r_0$, requirement (25) is implied by

$$c_0 \left(1 + \frac{r\rho}{2} \cdot c_0 c_1\right) \leq 1,$$

or equivalently

$$c_1 \leq \frac{1 - c_0}{\frac{r\rho}{2} c_0^2}. \quad (26)$$

Also notice that for constant $\sigma_i = \sigma$ we have $S'_1 = S_1 \sigma^2 / T$. Together with

$$\frac{S_1^2}{S_2} = \frac{\hat{S}_1^2}{\hat{S}_2} T \leq \hat{\rho} T$$

we obtain from (24)

$$\lambda + 1 \leq \frac{c_0 c_1}{2} \frac{S_1 S'_1}{S_2} \leq \frac{c_0 c_1}{2} \hat{\rho} \sigma^2. \quad (27)$$

Generally, if

$$c_1 \leq \frac{2}{\hat{\rho} c_0}, \quad (28)$$

then (27) implies $\lambda \leq \sigma^2$: Hence, (a) for our choice of u_0 and u_1 in this theorem, $U_0(\lambda) \leq u_0$ and $U_1(\lambda) \leq u_1$ as defined in Lemma 1, and (b) the condition $\lambda \leq \sigma_i^2 \ln \frac{N_c}{s_{i,c} \sigma_i}$ is satisfied (by assumption, $\frac{N_c}{s_{i,c} \sigma_i} \geq 1/r_0 \geq e$). This implies that Lemma 1 is indeed applicable.

For the above reasons we strengthen the requirement on ϵ (conditions (26) and (28) with (23)) to

$$\epsilon \leq \min \left\{ \frac{1 - c_0}{\frac{r\rho}{2} c_0^2}, \frac{2}{\hat{\rho} c_0} \right\} \cdot S_1 S'_1$$

For constant $\sigma_i = \sigma$, we have

$$S_1 S'_1 = T \hat{S}_1^2,$$

hence, we need

$$\epsilon \leq \min \left\{ \frac{1 - c_0}{\frac{r\rho}{2} c_0^2}, \frac{2}{\hat{\rho} c_0} \right\} \cdot T \hat{S}_1^2 \quad (29)$$

Summarizing (29), (21), and (20) for some positive integer λ proves (ϵ, δ) -differential privacy.

Condition (20) (i.e., $\exp(-\lambda\epsilon/2) \leq \delta$) is equivalent to

$$\ln(1/\delta) \leq \frac{\lambda\epsilon}{2} \quad (30)$$

If

$$\lambda = \lfloor c_0 \frac{\epsilon}{2S_2} \rfloor - 1 \quad (31)$$

is positive, then it satisfies (21) and we may use this λ in (30). This yields the condition

$$\ln(1/\delta) \leq \left(\lfloor c_0 \frac{\epsilon}{2S_2} \rfloor - 1 \right) \frac{\epsilon}{2},$$

which is implied by

$$\ln(1/\delta) \leq \left(c_0 \frac{\epsilon}{2S_2} - 2 \right) \frac{\epsilon}{2} = \frac{c_0}{4S_2} \epsilon^2 - \epsilon.$$

For constant $\sigma_i = \sigma$ we have $S_2 = \hat{S}_2 T / \sigma^2$ and the latter inequality is equivalent to

$$\sigma \geq \frac{2}{\sqrt{c_0}} \frac{\sqrt{\hat{S}_2} \sqrt{T(\epsilon + \ln(1/\delta))}}{\epsilon}. \quad (32)$$

Summarizing, if (29), (32), and the lambda value (31) is positive, then this shows (ϵ, δ) -differential privacy.

The condition (31) being positive follows from

$$\frac{4S_2}{c_0} \leq \epsilon.$$

Substituting $S_2 = \hat{S}_2 T / \sigma^2$ yields the equivalent condition

$$\frac{4T\hat{S}_2}{\sigma^2 c_0} \leq \epsilon$$

or

$$\sigma \geq \frac{2}{\sqrt{c_0}} \sqrt{\hat{S}_2} \frac{\sqrt{T\epsilon}}{\epsilon},$$

which is implied by (32). Summarizing, if (29) and (32), then this shows (ϵ, δ) -differential privacy. Notice that (32) corresponds to Theorem 1 in [Abadi et al., 2016] where all s_i are constant implying $\sqrt{\hat{S}_2} = q/\sqrt{1-q}$.

We are interested in a slightly different formulation: Given

$$c_1 = \min \left\{ \frac{1-c_0}{\frac{r\rho}{2}c_0^2}, \frac{2}{\hat{\rho}c_0} \right\}$$

what is the maximum possible c_0 (which minimizes σ implying more fast convergence to an accurate solution). We need to satisfy $c_0 \leq 2/(\hat{\rho}c_1)$ and

$$\frac{r\rho}{2}c_1c_0^2 + c_0 - 1 \leq 0,$$

that is,

$$(c_0 + 1/(r\rho c_1))^2 \leq 1/\left(\frac{r\rho}{2}c_1\right) + 1/(r\rho c_1)^2,$$

or

$$c_0 \leq \sqrt{1/\left(\frac{r\rho}{2}c_1\right) + 1/(r\rho c_1)^2} - 1/(r\rho c_1) = \frac{\sqrt{2r\rho c_1 + 1} - 1}{r\rho c_1}.$$

We have

$$c_0 = \min \left\{ \frac{\sqrt{2r\rho c_1 + 1} - 1}{r\rho c_1}, 2/(\hat{\rho}c_1) \right\} = c(c_1).$$

This finishes the proof.

B.3 Proof of Theorem 2

We will now analyse the requirements stated in Theorem 3. We will focus on the case where $c(x) = \frac{2}{\hat{\rho}x}$, which turns out to lead to practical parameter settings as discussed in the main body of the paper.

Requirement on r – (35): In Theorem 3 we use

$$r = r_0 \cdot 2^3 \cdot \left(\frac{1}{1-u_0} + \frac{1}{1-u_1} \frac{e^3}{\sigma^3} \right) e^{3/\sigma^2}$$

with

$$u_0 = \frac{2\sqrt{r_0\sigma}}{\sigma - r_0} \text{ and } u_1 = \frac{2e\sqrt{r_0\sigma}}{(\sigma - r_0)\sigma},$$

where r_0 is such that it satisfies

$$r_0 \leq 1/e, \quad u_0 < 1, \text{ and } u_1 < 1. \quad (33)$$

In our application of Theorem 3 we substitute $r_0 = \alpha\sigma$. This translates the requirements of (33) into

$$\alpha \leq \frac{1}{e\sigma}, \quad \alpha < 1, \text{ and } \sigma > \frac{2e\sqrt{\alpha}}{1-\alpha}. \quad (34)$$

As we will see in our derivation, we will require another lower bound (39) on σ . We will use (39) together with

$$\alpha \leq \frac{1}{e\sqrt{2(\epsilon + \ln(1/\delta))/\epsilon}}, \quad \alpha < 1, \text{ and } \sqrt{2(\epsilon + \ln(1/\delta))/\epsilon} > \frac{2e\sqrt{\alpha}}{1-\alpha}$$

to imply the needed requirement (34). These new bounds on α are in turn equivalent to

$$\alpha \leq g(\epsilon, \delta) \text{ where} \tag{35}$$

$$g(\epsilon, \delta) = \min \left\{ \frac{\sqrt{\epsilon}}{e\sqrt{2(\epsilon + \ln(1/\delta))}}, \left(\sqrt{1 + \frac{e^2\epsilon}{2(\epsilon + \ln(1/\delta))}} - \frac{e\sqrt{\epsilon}}{\sqrt{2(\epsilon + \ln(1/\delta))}/\epsilon} \right)^2 \right\}$$

(notice that this implies $\alpha < 1$).

Substituting $r_0 = \alpha\sigma$ in the formula for r yields the expression

$$r = 2^3 \cdot \left(\frac{\sigma}{(1 - \sqrt{\alpha})^2} + \frac{1}{\sigma(1 - \alpha) - 2e\sqrt{\alpha}\sigma} \frac{e^3}{\sigma} \right) \cdot e^{3/\sigma^2} (1 - \alpha)\alpha. \tag{36}$$

Requirement on s_i/N – (37): In Theorem 3 we also require $s_i/N \leq r_0/\sigma$ which translates into

$$s_i/N \leq \alpha. \tag{37}$$

Requirement on σ – (39) and (40): In Theorem 3 we restrict ourselves to the case where function $c(x)$ attains the minimum $c(x) = 2/(\hat{\rho}x)$. This happens when

$$\frac{\sqrt{2r\rho x + 1} - 1}{r\rho x} \geq \frac{2}{\hat{\rho}x}.$$

This is equivalent to

$$x \geq 2r \frac{\rho}{\hat{\rho}^2} + \frac{2}{\hat{\rho}}. \tag{38}$$

Notice that in the lower bound for σ in Theorem 3 we use $c_0 = c(x)$ for $x = c_1$, where c_1 is implicitly defined by

$$\epsilon = c_1 T \hat{S}_1^2$$

or equivalently

$$c_1 = \frac{\epsilon}{T \hat{S}_1^2}.$$

To minimize ϵ , we want to minimize $c_1 = x$. That is, we want $c_1 = x$ to match the lower bound (38). This lower bound is smallest if we choose the smallest possible ρ (due to the linear dependency of the lower bound on ρ). Given the constraint on ρ this means we choose

$$\rho = \frac{\hat{S}_1 \hat{S}_3}{\hat{S}_2^2}.$$

For $c_1 = x$ satisfying (38) we have

$$c_0 = c(c_1) = \frac{2}{\hat{\rho}x}.$$

Substituting this in the lower bound for σ attains

$$\sigma \geq \frac{2}{\sqrt{c(c_1)}} \frac{\sqrt{\hat{S}_2 T (\epsilon + \ln(1/\delta))}}{\epsilon} = \sqrt{\frac{\hat{\rho} \hat{S}_2}{\hat{S}_1^2}} \sqrt{2(\epsilon + \ln(1/\delta))/\epsilon}.$$

In order to yield the best test accuracy we want to choose the smallest possible σ . Hence, we want to minimize the lower bound for σ and therefore choose the smallest $\hat{\rho}$ given its constraints, i.e.,

$$\hat{\rho} = \frac{\hat{S}_1^2}{\hat{S}_2}.$$

This gives

$$\sigma \geq \sqrt{2(\epsilon + \ln(1/\delta))/\epsilon}. \tag{39}$$

Notice that this lower bound implies $\sigma \geq 216/215$ and for this reason we do not state this as an extra requirement.

Our expressions for ρ , $\hat{\rho}$, and c_1 with $x = c_1$ shows that lower bound (38) holds if and only if

$$\epsilon \geq \left(2r \frac{\hat{S}_3}{\hat{S}_1} + 2\hat{S}_2 \right) T. \tag{40}$$

Requirement implying (40): The definition of moments \hat{S}_j imply

$$\hat{S}_1 = \frac{K}{TN}$$

and, since $s_i/N \leq \alpha < 1$,

$$\hat{S}_j \leq \alpha^j / (1 - \alpha)^{j-1}.$$

Lower bound (40) on ϵ is therefore implied by

$$\epsilon \geq 2r \frac{\alpha^3}{(1 - \alpha)^2} \frac{T^2 N}{K} + 2 \frac{\alpha^2}{1 - \alpha} T. \quad (41)$$

We substitute

$$T = \beta \frac{K}{N} \quad (42)$$

in (41) which yields the requirement

$$\epsilon \frac{N}{K} \geq \frac{2r}{\alpha(1 - \alpha)^2} (\alpha^2 \beta)^2 + \frac{2}{1 - \alpha} (\alpha^2 \beta). \quad (43)$$

This inequality is implied by the combination of the following two inequalities:

$$\alpha^2 \beta \leq \frac{\epsilon N}{\gamma K} \quad (44)$$

and

$$1 \geq \frac{2r}{\alpha(1 - \alpha)^2} \frac{\epsilon N}{K} \frac{1}{\gamma^2} + \frac{2}{1 - \alpha} \frac{1}{\gamma}. \quad (45)$$

Inequality (45) is equivalent to

$$\gamma \geq \frac{2r}{\alpha(1 - \alpha)^2} \frac{\epsilon N}{\gamma K} + \frac{2}{1 - \alpha}. \quad (46)$$

This implies

$$\gamma \geq \frac{2}{1 - \alpha} \geq 2.$$

Also notice that

$$\frac{1}{\beta} = \frac{K}{TN} = \hat{S}_1 \leq \alpha$$

from which we obtain

$$1 \leq \alpha \beta.$$

Let us define

$$\bar{\alpha} = \frac{\epsilon N}{\gamma K}. \quad (47)$$

Inequalities $\gamma \geq 2$ and $1 \leq \alpha \beta$ together with (44) and the definition of $\bar{\alpha}$ imply

$$\alpha \leq \alpha^2 \beta \leq \frac{\epsilon N}{\gamma K} = \bar{\alpha} \leq \frac{\epsilon N}{2K}. \quad (48)$$

We will require

$$\bar{\alpha} < 1 \quad (49)$$

and also $\sigma(1 - \bar{\alpha}) - 2e\sqrt{\bar{\alpha}} > 0$ i.e.,

$$\sigma > \frac{2e\sqrt{\bar{\alpha}}}{1 - \bar{\alpha}}. \quad (50)$$

Bounds (49) and (50) are equivalent to

$$\bar{\alpha} \leq h(\sigma) \text{ where } h(\sigma) = \left(\sqrt{1 + (e/\sigma)^2} - e/\sigma \right)^2. \quad (51)$$

With condition (51) in place we may derive the upper bound

$$\begin{aligned} & \frac{2r}{\alpha(1-\alpha)^2} \\ = & \frac{2^4}{1-\alpha} \left(\frac{\sigma}{(1-\sqrt{\alpha})^2} + \frac{1}{\sigma(1-\alpha) - 2e\sqrt{\alpha}} \frac{e^3}{\sigma} \right) e^{3/\sigma^2} \\ \leq & \frac{2^4}{1-\bar{\alpha}} \left(\frac{\sigma}{(1-\sqrt{\bar{\alpha}})^2} + \frac{1}{\sigma(1-\bar{\alpha}) - 2e\sqrt{\bar{\alpha}}} \frac{e^3}{\sigma} \right) e^{3/\sigma^2} \end{aligned}$$

because all denominators are decreasing functions in α and remain positive for $\alpha \leq \bar{\alpha}$. Similarly,

$$\frac{2}{1-\alpha} \leq \frac{2}{1-\bar{\alpha}}.$$

These two upper bounds combined with (47) show that (46) is implied by choosing

$$\gamma = \gamma(\sigma, \epsilon N/K),$$

where $\gamma(\sigma, \epsilon N/K)$ is defined as the smallest solution of γ satisfying

$$\begin{aligned} \gamma & \geq \frac{2}{1-\bar{\alpha}} + \\ & \frac{2^4 \cdot \bar{\alpha}}{1-\bar{\alpha}} \left(\frac{\sigma}{(1-\sqrt{\bar{\alpha}})^2} + \frac{1}{\sigma(1-\bar{\alpha}) - 2e\sqrt{\bar{\alpha}}} \frac{e^3}{\sigma} \right) e^{3/\sigma^2}, \end{aligned} \tag{52}$$

where $\bar{\alpha} = (\epsilon N/K)/\gamma$. The smallest solution γ will meet (52) with equality. For this reason the minimal solution γ will be at most the right hand side of (52) where γ is replaced by its lower bound 2; this is allowed because this increases $\bar{\alpha}$ to the upper bound in (48) and we know that the right hand side of (52) increases in $\bar{\alpha}$ up to the upper bound in (48) if the upper bound satisfies

$$\frac{\epsilon N}{2K} \leq h(\sigma).$$

This makes requirement (51) slightly stronger – but in practice this stronger requirement is already satisfied because K is several epochs of N iterations making $\frac{\epsilon N}{2K} \ll 1$ while $\sigma \gg 1$ for small ϵ implying that $h(\sigma)$ is close to 1.

Notice that $\gamma = 2 + O(\bar{\alpha})$, hence, for small $\bar{\alpha}$ we have $\gamma \approx 2$. A more precise asymptotic analysis reveals

$$\gamma = 2 + (2 + 2^4 \cdot \left(\sigma + \frac{e^3}{\sigma^2} \right) e^{3/\sigma^2}) \bar{\alpha} + O(\bar{\alpha}^{3/2}).$$

Relatively large $\bar{\alpha}$ closer to 1 will yield $\gamma \gg 2$.

Summarizing

$$\{(42), (44), (47), (51), (52)\} \Rightarrow (40).$$

Combining all requirements – resulting in (54), (55), and (39), or equivalently (57), (58), and (39): The combination of requirements (42) and (44) is equivalent to

$$\alpha \leq \sqrt{\frac{\epsilon}{\gamma T}} \tag{53}$$

(notice that T and β are not involved in any of the other requirements including those discussed earlier in this discussion, hence, we can discard (42) and substitute this in (44)). The combination of (47), (51), and (52) is equivalent to

$$\frac{\epsilon N}{\gamma K} \leq h(\sigma) \text{ with } \gamma = \gamma \left(\sigma, \frac{\epsilon N}{K} \right) \tag{54}$$

(for the definition of $h(\cdot)$ see (51) and for $\gamma(\cdot, \cdot)$ see (52)).

We may now combine (53), (35), and (37) into a single requirement

$$s_i/N \leq \min \left\{ g(\epsilon, \delta), \sqrt{\frac{\epsilon}{\gamma T}} \right\} \tag{55}$$

(for the definition of $g(\cdot, \cdot)$ see (35)). This shows that (54), (55), and (39) (we remind the reader that the last condition is the lower bound on $\sigma \geq \sqrt{2(\epsilon + \ln(1/\delta))/\epsilon}$) implies (ϵ, δ) -DP by Theorem 3.

Let us rewrite these conditions. We introduce the mean \bar{s} of all s_i defined by

$$\bar{s} = \frac{1}{T} \sum_{i=0}^{T-1} s_i = \frac{K}{T}$$

and we introduce the maximum s_{max} of all s_i defined by

$$s_{max} = \max\{s_0, \dots, s_{T-1}\}.$$

We define θ as the fraction

$$\theta = \frac{s_{max}}{\bar{s}}. \tag{56}$$

This notation allows us to rewrite

$$s_i/N \leq \sqrt{\frac{\epsilon}{\gamma T}}$$

from (55) as

$$\gamma \frac{K}{N} \frac{\bar{s}}{N} \theta^2 \leq \epsilon.$$

From this we obtain that the requirements (54) and (55) are equivalent to

$$\gamma \left(\sigma, \frac{\epsilon N}{K} \right) \cdot \frac{K}{N} \frac{\bar{s}}{N} \theta^2 \leq \epsilon \leq \gamma \left(\sigma, \frac{\epsilon N}{K} \right) \cdot h(\sigma) \frac{K}{N} \tag{57}$$

and

$$\theta \bar{s} \leq g(\epsilon, \delta) N. \tag{58}$$

This alternative description shows that (57), (58), and (39) with definitions for $h(\cdot)$, $\gamma(\cdot, \cdot)$, $g(\cdot, \cdot)$, and θ in (51), (52), (35), and (56) implies (ϵ, δ) -DP. This proves Theorem 2 (after a slight rewrite of the definitions of functions $h(\cdot)$ and $g(\cdot, \cdot)$).

C Experiments

We provide experiments to support our theoretical findings, i.e., convergence of our proposed asynchronous distributed learning framework with differential privacy (DP) to a sufficiently accurate solution. We cover strongly convex, plain convex and non-convex objective functions over iid local data sets.

We introduce our experimental set up in Section C.1. Section C.2 provides utility graphs for different data sets and objective functions. A utility graph helps choosing the maximum possible noise σ , in relation to the value of the clipping constant C , for which decent accuracy can be achieved. Section C.3 provides detailed experiments for our asynchronous differential privacy SGD framework (asynchronous DP-SGD) with different types of objective functions (i.e., strongly convex, plain convex and non-convex objective functions), different types of constant sample size sequences and different levels of privacy guarantees (i.e., different privacy budgets ϵ).

All our experiments are conducted on LIBSVM [Chang and Lin, 2011][¶] and MNIST [LeCun and Cortes, 2010]^{||} data sets.

C.1 Experiment settings

Simulation environment. For simulating the asynchronous DP-SGD framework, we use multiple threads where each thread represents one compute node joining the training process. The experiments are conducted on Linux-64bit OS, with 16 cpu processors, and 32Gb RAM.

Objective functions. Equation (59) defines the plain convex logistic regression problem. The weight vector w and the bias value b of the logistic function can be learned by minimizing the log-likelihood function J :

$$J = - \sum_{i=1}^N [y_i \cdot \log(\bar{\sigma}_i) + (1 - y_i) \cdot \log(1 - \bar{\sigma}_i)], \text{ (plain convex)} \quad (59)$$

where N is the number of training samples (x_i, y_i) with $y_i \in \{0, 1\}$ and $\bar{\sigma}_i$ is defined by

$$\bar{\sigma}_i = \frac{1}{1 + e^{-(w^T x_i + b)}},$$

which is the sigmoid function with parameters w and b . Our goal is to learn a vector w^* which represents a pair $\bar{w} = (w, b)$ that minimizes J .

Function J can be changed into a strongly convex problem \hat{J} by adding a regularization parameter $\lambda > 0$:

$$\hat{J} = - \sum_{i=1}^N [y_i \cdot \log(\sigma_i) + (1 - y_i) \cdot \log(1 - \sigma_i)] + \frac{\lambda}{2} \|w\|^2, \text{ (strongly convex).}$$

where $\bar{w} = (w, b)$ is vector w concatenated with bias value b . In practice, the regularization parameter λ is set to $1/N$ [Roux et al., 2012].

For simulating non-convex problems, we choose a simple neural network (Letnet) [LeCun et al., 1998] with cross entropy loss function for image classification.

The loss functions for the strong, plain, and non-convex problems represent the objective function $F(\cdot)$.

Parameter selection. The parameters used for our distributed algorithm with Gaussian based differential privacy for strongly convex, plain convex and non-convex objective functions are described in Table 1. The clipping constant C is set to 0.1 for strongly convex and plain convex problems and 0.025 for non-convex problem (this turns out to provide good utility).

For the plain convex case, we can use diminishing step size schemes $\frac{\eta_0}{1+\beta \cdot t}$ or $\frac{\eta_0}{1+\beta \cdot \sqrt{t}}$. In this paper, we focus our experiments for the plain convex case on $\frac{\eta_0}{1+\beta \cdot \sqrt{t}}$. Here, η_0 is the initial step size and we perform a systematic grid search on parameter $\beta = 0.001$ for strongly convex case and $\beta = 0.01$ for both plain convex and non-convex cases. Moreover, most of the experiments are conducted with 5 compute nodes and 1 central server. When we talk about accuracy (from Figure 7 and onward), we mean test accuracy defined as the fraction of samples from a test data set that get accurately labeled by the classifier (as a result of training on a training data set by minimizing a corresponding objective function).

[¶]<https://www.csie.ntu.edu.tw/~cjlin/libsvmtools/datasets/binary.html>

^{||}<http://yann.lecun.com/exdb/mnist/>

Table 1: Common parameters of asynchronous DP-SGD framework with differential privacy

	# of clients n	Diminishing step size $\bar{\eta}_t$	Regular λ	Clipping constant C
Strongly convex	5	$\frac{\eta_0}{1+\beta t}$ [‡]	$\frac{1}{N}$	0.1
Plain convex	5	$\frac{\eta_0}{1+\beta t}$ or $\frac{\eta_0}{1+\beta\sqrt{t}}$	N/A	0.1
Non-convex	5	$\frac{\eta_0}{1+\beta\sqrt{t}}$	N/A	0.025

[‡] The i -th round step size $\bar{\eta}_i$ is computed by substituting $t = \sum_{j=0}^{i-1} s_j$ into the diminishing step size formula.

C.2 Utility graph

The purpose of a utility graph is to help us choose, given the value of the clipping constant C , the maximum possible noise σ for which decent accuracy can be achieved. A utility graph depicts the test accuracy of model $F(w^* + n)$ over $F(w^*)$, where w^* is a near optimal global model and $n \sim \mathcal{N}(0, C^2\sigma^2\mathbf{I})$ is Gaussian noise. This shows which maximum σ can be chosen with respect to allowed loss in expected test accuracy, clipping constant C and standard deviation σ .

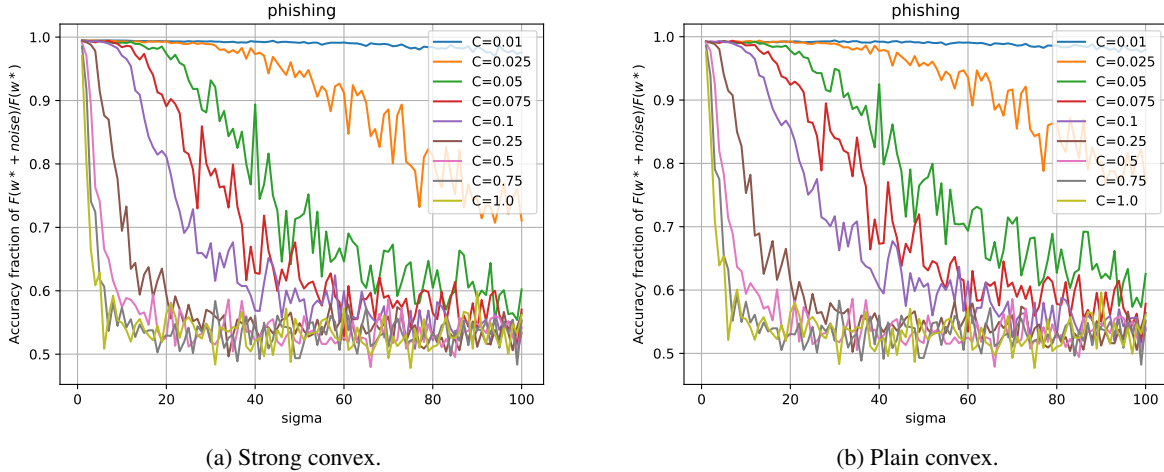


Figure 4: Utility graph with various gradient norm C and noise level σ

As can be seen from Figure 4 and Figure 5, for clipping constant $C = 0.1$, we can choose the maximum σ somewhere in the range $\sigma \in [18, 22]$ if we want to guarantee there is at most about 10% accuracy loss compared to the (near)-optimal solution without noise. Another option is $C = 0.075$, where we can tolerate $\sigma \in [18, 30]$ yielding the same accuracy loss guarantee. When the gradient bound C gets smaller, our DP-SGD can tolerate bigger noise, i.e, bigger values of σ . However, we need to increase the number K of iterations during the training process when C is smaller in order to converge and gain a specific test accuracy – this is the trade-off. For simplicity, we intentionally choose $C = 0.1$, $\sigma \leq 20$ and expected test accuracy loss about 10% for our experiments with strongly convex and plain convex objective functions.

The utility graph is extended to the non-convex objective function in Figure 6. To keep the test accuracy loss less or equal to 10% (of the final test accuracy of the original model w^*), we choose $C = 0.025$ and noise level $\sigma \leq 12$. For simplicity, we use this parameter setting for our experiments with the non-convex problem.

C.3 Asynchronous distributed learning with differential privacy

We consider the asynchronous DP-SGD framework with strongly convex, plain convex and non-convex objective functions for different settings, i.e., different levels of privacy budget ϵ and different constant sample size sequences.

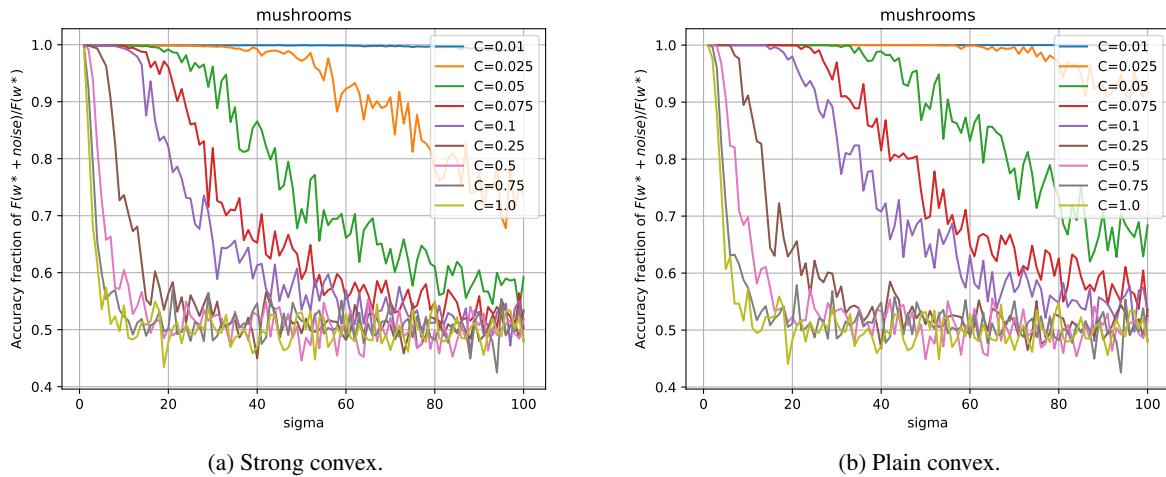


Figure 5: Utility graph with various gradient norm C and noise level σ

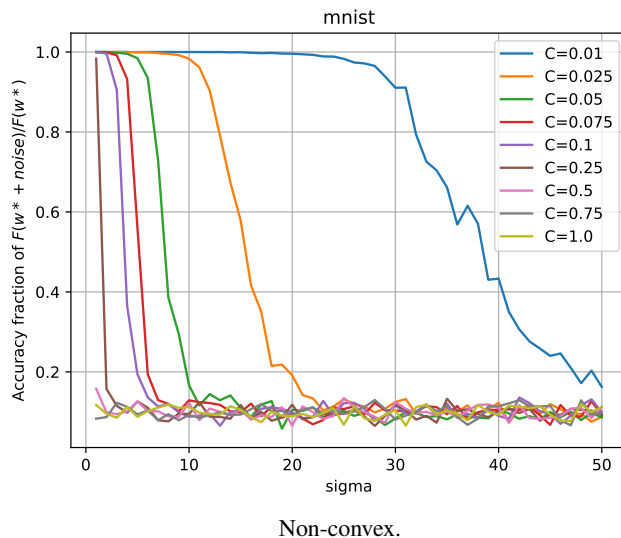


Figure 6: Utility graph with various gradient norm C and noise level σ

C.3.1 Asynchronous DP-SGD with different constant sample size sequences

The purpose of this experiment is to investigate which is the best constant sample size sequence $s_i = s$. This experiment allows us to choose a decent sample size sequence that will be used in our subsequent experiments. To make the analysis simple, we consider our asynchronous DP-SGD framework with $\Upsilon(k, i)$ defined as false if and only if $k < i - 1$, i.e., compute nodes are allowed to run fast and/or have small communication latency such that broadcast global models are at most 1 local round in time behind (so different clients can be asynchronous with respect to one another for 1 local round). We also use iid data sets. The detailed parameters are in Table 2.

The results from Figure 7 to Figure 8 confirm that our asynchronous DP-SGD framework can converge under a very small privacy budget. When the constant sample size $s = 1$, it is clear that the DP-SGD algorithm does not achieve good accuracy compared to other constant sample sizes even though this setting has the maximum number of communication rounds. When we choose constant sample size $s = 26$ (this meets the upper bound for constant sample sizes for our small $N = 10,000$ and small $\epsilon \approx 0.05$, see Theorem 2), our DP-SGD framework converges to a decent test accuracy, i.e., the test accuracy loss is expected less than or equal to 10% when compared to the original mini-batch SGD without noise. In conclusion, this experiment demonstrates that our asynchronous DP-SGD with diminishing step size scheme

Table 2: Basic parameter setting for strongly and plain convex problems

Parameter	Value	Note
$\bar{\eta}_0$	0.1	initial stepsize
N_c	10,000	# of data points
K	50,000	# of iterations
ϵ	0.04945	
σ	19.29962	
δ	0.0001	
C	0.1	clipping constant
s	$\{1, 5, 10, 15, 20, 26\}$	constant sample size sequence
dataset	LIBSVM	iid dataset
n	5	# of nodes
Υ	$k \geq i - 1$	1-asynchronous round

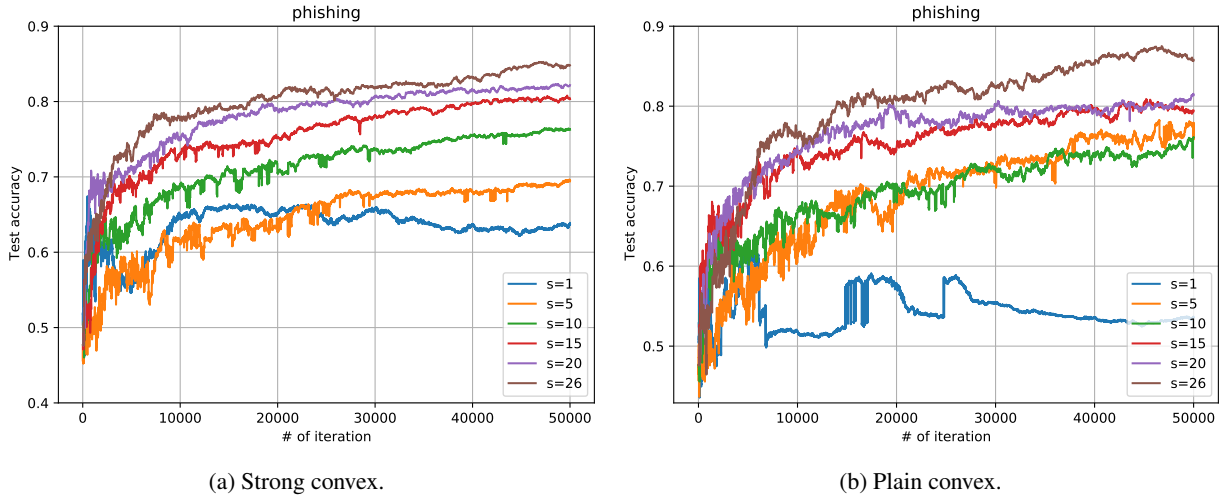


Figure 7: Effect of different constant sample size sequences

and constant sample size sequence works well under DP setting, i.e. our asynchronous DP-SGD framework can gain differential privacy guarantees while maintaining an acceptable accuracy.

Table 3: Basic parameter setting for non-convex problem

Parameter	Value	Note
$\bar{\eta}_0$	0.1	initial stepsize
N_c	60,000	# of data points
K	360,000	# of iterations
ϵ	0.15007	
σ	12.10881	
δ	$1.667 \cdot 10^{-5}$	
C	0.025	clipping constant
s	$\{10, 25, 50, 100, 200, 300, 370\}$	constant sample size sequence
dataset	MNIST	iid dataset
n	5	# of nodes
Υ	$k \geq i - 1$	1-asynchronous round

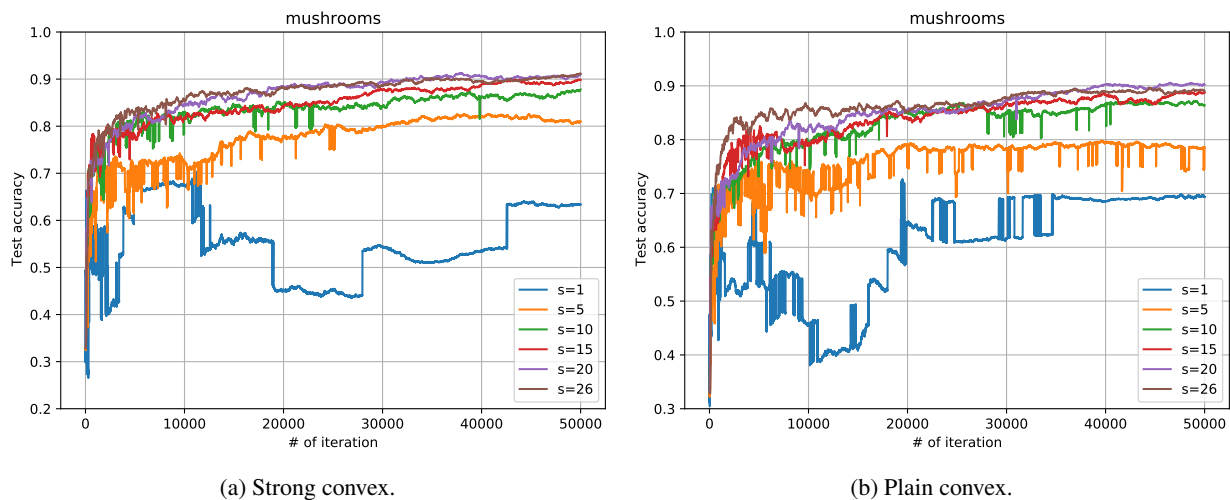


Figure 8: Effect of different constant sample size sequences

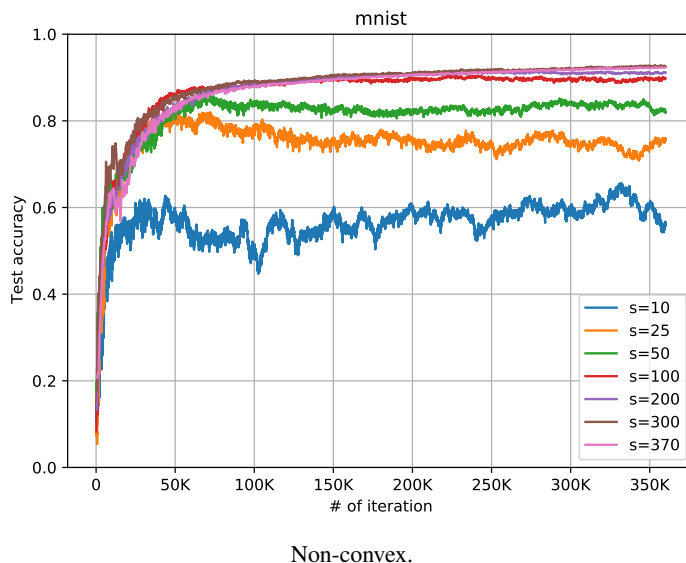


Figure 9: Effect of different constant sample size sequences

We also conduct the experiment for the non-convex objective function. The detailed parameter settings can be found in Table 3. Here, we again consider our asynchronous setting where each compute node is allowed to run fast and/or has small communication latency such that broadcast global models are at most 1 local round in time behind. As can be seen from Figure 9, our proposed asynchronous DP-SGD still converges under small privacy budget. Moreover, when we use the constant sample size $s = 370$ (this meets the upper bound for constant sample sizes for our small $N = 60,000$ and small $\epsilon \approx 0.15$, see Theorem 2), we can significantly reduce the communication cost compared to other constant sample sizes while keeping the test accuracy loss within 10%. The constant sample size $s = 10$ (as well as $s \leq 10$) shows a worse performance while this setting requires more communication rounds, compared to other constant sample sizes. This figure again confirms the effectiveness of our asynchronous DP-SGD framework towards a strong privacy guarantee for all types of objective function.

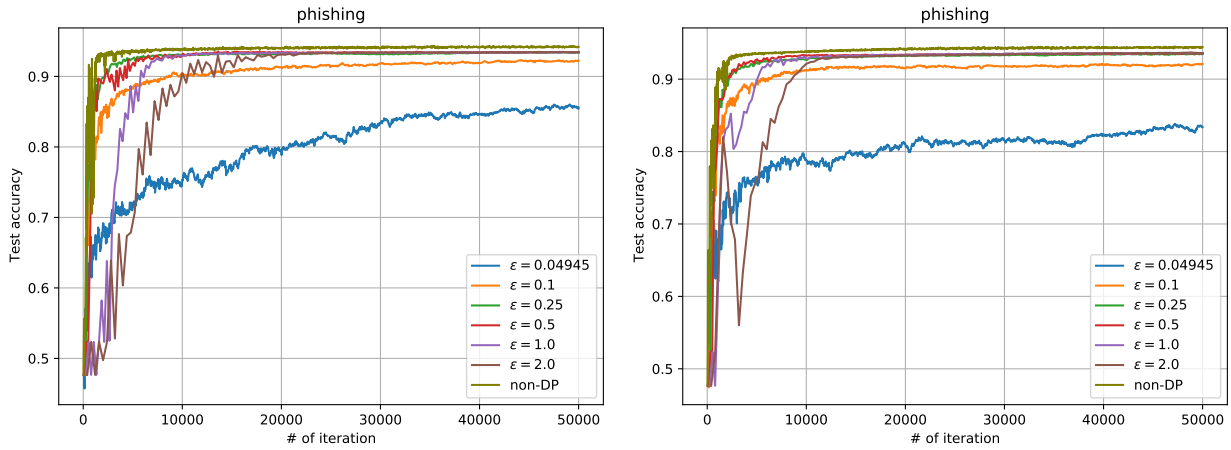
C.3.2 Asynchronous DP-SGD with different levels of privacy budget

We conduct the following experiments to compare the effect of our DP-SGD framework for different levels of privacy budget ϵ including the non-DP setting (i.e., no privacy at all, hence, no noise). The purpose of this experiment is to show

Table 4: Different privacy budget settings for strongly and plain convex problems

Privacy budget (ϵ, δ)	σ	Sample size s
$(0.04945, 0.0001)$	19.29962	26
$(0.1, 0.0001)$	13.06742	55
$(0.25, 0.0001)$	8.59143	103
$(0.5, 0.0001)$	6.05868	168
$(1.0, 0.0001)$	4.27273	265
$(2.0, 0.0001)$	3.03241	400

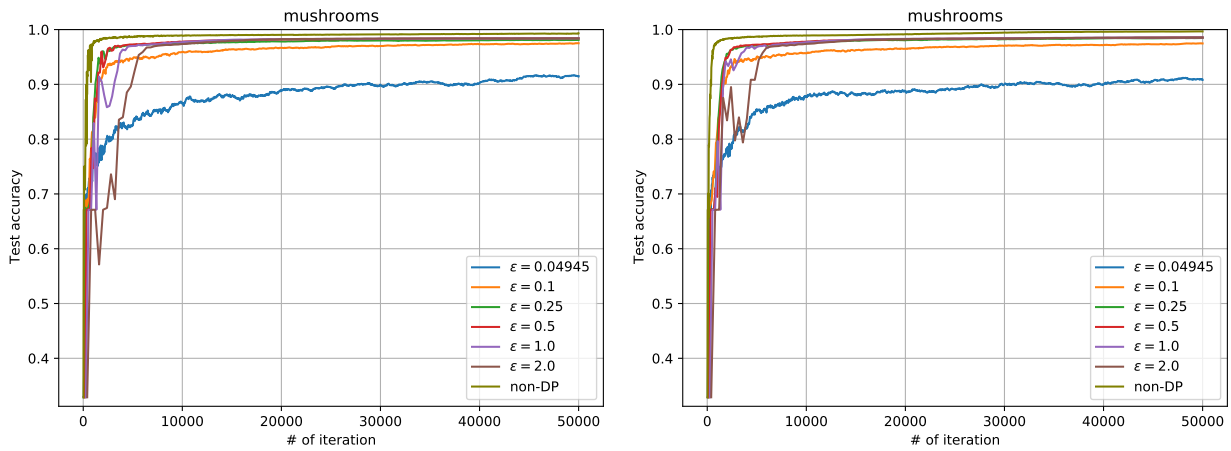
that the test accuracy degradation is at most 10% even if we use very small ϵ . The detailed constant sample sequence s and noise level σ based on Theorem 2 are illustrated in Table 4. Other parameter settings, such as initial stepsize η_0 , are kept the same as in Table 2.



(a) Strong convex.

(b) Plain convex.

Figure 10: Effect of different levels of privacy budgets ϵ and non-DP settings



(a) Strong convex.

(b) Plain convex.

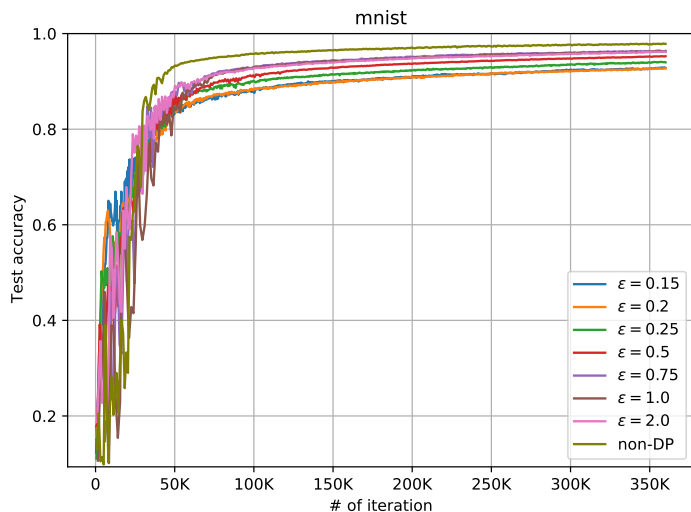
Figure 11: Effect of different levels of privacy budgets ϵ and non-DP settings

As can be seen from Figures 10 and Figure 11, the test accuracy degradation is about 10% for $\epsilon = 0.04945$ compared to the other graphed privacy settings and non-DP setting. Privacy budget $\epsilon = 0.1$, still significant smaller than what is reported in literature, comes very close to the maximum attainable test accuracy of the non-DP setting.

We ran the same experiment for the non-convex objective function. The detailed setting of different privacy budgets is shown in Table 5. Note that we also set the asynchronous behavior to be 1 asynchronous round, and the total of iterations on each compute node is $K = 360,000$. Other parameter settings for the non-convex case, such as initial stepsize η_0 , are kept the same as in Table 3. As can be seen from Figure 12, the test accuracy loss with $\epsilon \approx 0.15$ is less than 10% (the expected test accuracy degradation from utility graph at Figure 6).

Table 5: Different privacy budget settings for non-convex problem

Privacy budget (ϵ, δ)	σ	Sample size s
$(0.15007, 1.667 \cdot 10^{-5})$	12.10881	370
$(0.2, 1.667 \cdot 10^{-5})$	10.48452	460
$(0.25, 1.667 \cdot 10^{-5})$	9.37379	543
$(0.5, 1.667 \cdot 10^{-5})$	6.63120	889
$(0.75, 1.667 \cdot 10^{-5})$	5.41887	1168
$(1.0, 1.667 \cdot 10^{-5})$	4.69244	1409
$(2.0, 1.667 \cdot 10^{-5})$	3.31648	2159



Non-convex.

Figure 12: Effect of different levels of privacy budgets ϵ and non-DP settings

These figures again confirm the effective performance of our DP-SGD framework, which not only conserves strong privacy, but also keeps a decent convergence rate to good accuracy, even for a very small privacy budget.